UNIVERSIDADE DE LISBOA
FACULDADE DE CIÊNCIAS
DEPARTAMENTO DE BIOLOGIA ANIMAL

Plasmodium berghei liver infection inhibition by host immune response to *Trypanosoma brucei*

Rafael Alexandre Carvalho Luís

Mestrado em Biologia Humana e Ambiente

Dissertação orientada por:
Doutor Miguel Prudêncio
Professora Doutora Teresa Rebelo

2018

ACKNOWLEDGMENTS

Em primeiro lugar, um obrigado enorme ao Miguel por me ter dado a oportunidade de pertencer ao laboratório! Todo o teu apoio, ajuda e motivação ao longo do projeto tornaram a minha passagem pelo Prudêncio Lab uma das experiências mais enriquecedoras que experienciei até agora. Aproveito ainda para te dizer que trabalhar contigo foi um orgulho e um privilégio!

Obrigado também a ti, Margarida! Por me ensinares tanto do que é ser um cientista, por toda a paciência que tiveste comigo ao longo do ano e por toda a dedicação que mostraste. Ambos sabemos que nem sempre foi um "mar de rosas", mas ainda assim acho sem qualquer dúvida que éramos uma dupla de trabalho excelente!

E como a Margarida me dizia "Não te esqueças que dois parasitas envolvem dois laboratórios!", não me posso esquecer de te agradecer, Luísa! Obrigado pela motivação e pelas "perguntas difíceis" que me deixavam a pensar. Apesar de não ser oficialmente parte do laboratório, obrigado pela oportunidade que me deste de integrá-lo!

Obrigado também à Professora Teresa Rebelo e à Professora Deodália Dias pela preocupação e disponibilidade que demonstraram ao longo de todo o Mestrado!

Com isto dito, tenho de agradecer também a quem me aturava todos os dias! Aos Prudêncios: António, Denise, Filipa, Fontinha, Francisca, Helena, Patrícia e Raquel. Um obrigado gigante pelo apoio, esclarecimento de dúvidas (tanto científicas como existenciais!) e disponibilidade que demonstraram ao longo deste ano. Sem vocês este percurso não tinha sido de todo tão bom. São fantásticos! Mas ainda faltam alguns Prudêncios… Um obrigado muito especial à Daniela, à Diana e ao Rafael (Chefe). Todo o companheirismo e amizade que demonstraram, todos os desabafos, todos os almoços, "txica txicas", cafezinhos e lanches são algo que não me vou esquecer tão cedo. Foram e são espetaculares! Vamos continuar a bombar no "Muro"!

Também vocês, Figueiredos, me aturavam constantemente: Alexandra, Christina, Daniel, Fabien, Henrique, Idálio, João, Leonor, Tiago, Mariana, Miguel, Pena, Sandra. Um grande obrigado! Desde me abrirem portas ao fim-de-semana quando eu me esquecia do cartão, a ajudas em experiências e até desabafos, vocês nunca falharam!

Agora chegou a vez de quem me atura há anos.

Obrigado a ti, Diogo, por estares sempre presente e saberes sempre como me fazer tirar a cabeça do trabalho!

Obrigado Carolina, por me dizeres o que mais ninguém tem coragem! Obrigado pelos desabafos, pelos conselhos, por saberes sempre o que dizer… Acho que sabes perfeitamente o quanto me ajudaste ao longo deste tempo.

Aos meus afilhados: Alexandra, Beatriz, Catarina, Coutinho, Gonçalo, Margarida, Marta, Miguel, Renata e Zé. É com toda a Felicidade que aqui vos agradeço toda a preocupação, carinho, apoio, motivação, confiança e Força que me transmitiram. Mesmo não o sabendo, vocês foram responsáveis por grande parte do meu Esforço e Sucesso ao longo deste ano e tenho Sorte em ter-vos por perto. Obrigado.

Maria… A companhia de excelência para festa, música e dança. Um obrigado por me ires desencaminhando exatamente quando é preciso!

Um Obrigado também a todos os meus amigos cujo nome não está aqui escrito, mas que eu sei (e vocês sabem) que fizeram parte do meu percurso.

E como esta secção não seria verdadeira se não incluísse as pessoas mais importantes… Obrigado do fundo do coração aos meus pais, irmãs e padrinhos! Pela vossa compreensão. Pelo apoio e motivação. Por deixarem jantar feito quando era preciso. Pelas pequenas e grandes coisas que vos fazem ser a melhor família do Mundo! Sempre me deram mais do que aquilo que alguma vez conseguirei retribuir… Mas prometo que tentarei sempre fazê-lo. OBRIGADO.

ABSTRACT

Malaria and sleeping sickness are diseases that share overlapping spacial distributions in sub-Saharan Africa. Malaria is caused by *Plasmodium* parasites, while sleeping sickness is caused by *Trypanosoma brucei* parasites. Previous results from the host lab using a coinfection mouse model have shown that *P. berghei* hepatic infection is significantly inhibited by an ongoing *T. brucei* infection, an effect that is phenocopied by the injection of *T. brucei* lysates prior to inoculation of *P. berghei* sporozoites. Additional research suggested that the host's immune system mediates this impairment through an elimination of *P. berghei* sporozoites before their invasion of the hepatocytes and through an elimination of exoerythrocytic forms (EEFs) during an ongoing *P. berghei* infection.

In this thesis, we aimed at investigating the involvement of immune responses on the mechanisms by which *T. brucei* is able to impair a subsequent *P. berghei* hepatic infection. We showed that Interferon-γ (IFN-γ) deficient coinfected mice display a *P. berghei* hepatic infection at 6 hours post-sporozoite injection similar to that of IFN-γ-deficient mice infected solely with *P. berghei*, indicating that IFN-γ is an essential immune factor in the impairment of host hepatocyte invasion by *P. berghei* sporozoites in mice with an ongoing *T. brucei* infection. Nevertheless, the immune cells involved in the *T. brucei*-mediated impairment of *P. berghei* hepatocyte invasion remain to be elucidated. Since the immune system appeared to be involved in the impairment of *P. berghei* liver infection by *T. brucei*, we sought to understand if when *T. brucei* lysates are injected, a peak in immune response occurred, which would be followed by its continuous decrease, corresponding to the clearance of *T. brucei* molecules. Our work revealed that the protection conferred by *T. brucei* lysates is lost when the latter are injected 24 to 48 hours prior to sporozoite injection. Similarly to what was previously observed in the context of the coinfection, immunofluorescence microscopy analysis revealed that *T. brucei* lysates lead to the elimination of *P. berghei* parasites before reaching the liver or during the course of the liver stage of infection, without affecting their development. Considering that IFN-γ had been shown to play a role in *P. berghei* liver infection impairment in the context of coinfection, we sought to understand if cytokine profiles could be involved in the differential inhibitory effect of *T. brucei* lysates when injected at different timepoints. We determined the cytokine profiles at several timepoints of *P. berghei* infection in the serum from mice singly infected with *P. berghei*, coinfected mice, or mice injected with *T. brucei* lysates at several timepoints prior to *P. berghei* infection. Interestingly, we observed a correlation between monocyte chemoattractant protein-1 (MCP-1), macrophage inflammatory protein-1-alpha (MIP-1α) and interleukin-6 (IL-6) and the extent of *P. berghei* liver infection inhibition by *T. brucei*. Contrary to what we expected, even though MCP-1 and MIP-1α are chemotactic for macrophages and monocytes, depletion of macrophages and blockage of monocyte recruitment did not abrogate the impairment of *P. berghei* liver infection in coinfected mice.

Collectively, our results elucidate aspects of the biology of infection by *Trypanosoma* and *Plasmodium* parasites and unveil a potential role for IFN-γ in the elimination of *P. berghei* sporozoites prior to the invasion of hepatocytes. Furthermore, this work shows the possible involvement of cytokines in the impairment of *P. berghei* hepatic infection by *T. brucei*, revealing potential cytokine and chemokine mediators in the elimination of *P. berghei* EEFs.

KEYWORDS: malaria, *Plasmodium*, sleeping sickness, *Trypanosoma*, coinfection, immune system

RESUMO

A malária e a doença do sono são infeções tropicais cujas distribuições geográficas se sobrepõem em várias regiões do continente africano, em particular na África sub-Sahariana. Ambas estas doenças são causadas por parasitas com ciclos de vida complexos, envolvendo vários hospedeiros.

A malária é causada por parasitas do género *Plasmodium* que infetam hospedeiros mamíferos através da picada de um mosquito fêmea *Anopheles* infetado. Este injeta parasitas *Plasmodium* na forma de esporozoítos, os quais invadem a corrente sanguínea e migram para o fígado, onde infetam e se desenvolvem dentro de hepatócitos, originando formas exoeritrocitárias (EEFs). Apesar de assintomática, esta fase é obrigatória e culmina na libertação de merozoítos para a corrente sanguínea, os quais infetam eritrócitos, originando os sintomas da doença.

A doença do sono, ou Tripanossomíase Humana Africana, é causada pelo parasita *Trypanosoma brucei*, o qual é transmitido a um hospedeiro mamífero pela picada de uma mosca do género *Glossina*. Uma vez na corrente sanguínea, estes parasitas dividem-se e invadem outros órgãos, nomeadamente o tecido adiposo, que atua como um reservatório, e no cérebro, levando à disrupção do padrão sono-vigília, a maior característica desta doença.

Tendo em conta as regiões endémicas para malária e doença do sono, existem populações infetadas simultaneamente por ambos os parasitas, existindo já alguns relatórios que apontam para esta condição. Uma vez que existe uma notória escassez de conhecimento relativamente ao impacto de uma possível coinfecção entre estes parasitas no hospedeiro, é imperativa a realização de uma análise cuidada de possíveis efeitos resultantes da coinfecção entre *Plasmodium* e *Trypanosoma*.

Com o intuito de responder a esta necessidade, o laboratório de acolhimento realizou alguns estudos experimentais onde ratinhos foram submetidos a coinfecções entre *Plasmodium* e *Trypanosoma*. Os resultados mostraram que uma infeção primária por *T. brucei* conduz a uma inibição de cerca de 90% de uma infeção hepática subsequente por *P. berghei*. Experiências complementares revelaram que esta inibição é replicada pela injeção de lisados de *T. brucei* antes da infeção por *P. berghei*. Adicionalmente, experiências realizadas pelo laboratório indicam que é possível que a inibição da infeção hepática de *P. berghei* causada por *T. brucei* seja mediada pelo sistema imunitário do hospedeiro, tendo impacto tanto a nível do impedimento da invasão de hepatócitos pelos esporozoítos, bem como a nível da eliminação de EEFs durante a infeção. Como tal, esta dissertação pretende caracterizar o impacto da resposta imunitária a *T. brucei* que tem como consequência a inibição da infeção hepática de *P. berghei*.

Modelos *in vitro* providenciam oportunidades para estudar respostas celulares específicas num sistema fechado, onde as condições experimentais podem ser cuidadosamente controladas, sem existirem problemas éticos associados ao uso de modelos animais. Assim, a tentativa de estabelecimento de um sistema *in vitro* que fosse capaz de replicar o fenótipo observado em infeções de modelos animais foi o foco da nossa pesquisa. Para tal, combinámos esplenócitos e soro de ratinhos infetados com *T. brucei*, com um sistema *in vitro* previamente estabelecido. No nosso sistema, não nos foi possível observar diferenças na infeção hepática de *P. berghei* que fossem passíveis de serem atribuídas à combinação de componentes expostas a *T. brucei*, nomeadamente esplenócitos e soro de ratinhos infetados com *T. brucei*. De forma a tentar reproduzir mais fidedignamente o ambiente imunitário presente num hospedeiro, os nossos esforços foram alocados para a implementação de um sistema *in vitro* pioneiro baseado em cultura de seções de fígados de ratinho. A perda de viabilidade das seções revelou-se uma barreira intransponível com as metodologias disponíveis, o que se provou determinante na mudança do foco para a compreensão dos mecanismos de envolvimento do sistema imunitário do hospedeiro na coinfecção através da utilização de modelos murinos.

Experiências anteriores realizadas pelo laboratório de acolhimento mostraram que em modelos murinos incapazes de produzir células T e células B, existe uma recuperação de uma normal infeção hepática de *P. berghei* às 6 horas após injeção de esporozoítos, em ratinhos coinfetados com *T. brucei*

e *P. berghei*. De forma a tentar compreender o mecanismo imunitário responsável pela inibição da invasão hepática por *P. berghei* num hospedeiro previamente infetado com *T. brucei*, foram realizadas diversas experiências onde modelos animais incapazes de produzir diferentes tipos de células imunitárias foram utilizados. Os nossos resultados mostraram que a ausência de vários subtipos de células T não leva a uma recuperação de uma normal invasão de hepatócitos por parte dos esporozoítos de *P. berghei*. Também a ausência de células B não mostrou ter efeito no contexto de coinfecção, levando-nos a analisar o envolvimento de fatores imunitários no contexto da coinfecção. O interferão-γ (IFN-γ) destacou-se devido à sua estudada ação na eliminação de parasitas *Trypanosoma* e *Plasmodium* e, como tal, modelos murinos incapazes de produzir esta citocina foram empregues. Nesta experiência, foi possível observar uma recuperação total de uma infeção normal de *P. berghei* às 6 horas após injeção de esporozoítos em ratinhos coinfetados incapazes de produzir IFN-γ. Assim, concluímos que este fator é determinante no impedimento da invasão hepática por *P. berghei*, em hospedeiros infetados previamente com *T. brucei*.

Nesta dissertação, tentámos também avaliar a duração da proteção conferida pelos lisados de *T. brucei*, quando injetados antes de uma infeção com *P. berghei*. Para tal, lisados de *Trypanosoma* foram injetados a diferentes pontos no tempo antes da injeção de esporozoítos. Os dados obtidos revelaram que o efeito dos lisados de *T. brucei* é dependente do tempo de injeção dos lisados, sendo a proteção superior quando o tempo de injeção dos lisados é mais próximo do momento de infeção com *P. berghei*. De modo a esclarecer as causas da redução na infeção de *P. berghei* resultante da injeção de lisados de *T. brucei*, foi efetuada uma análise por microscopia de fluorescência que revelou um decréscimo no número de hepatócitos infetados. Porém, os parasitas que evadem esta eliminação inicial apresentam um crescimento semelhante ao dos parasitas em ratinhos infetados somente com *Plasmodium*.

Dada a dependência temporal do efeito dos lisados, e atendendo ao papel importante das citocinas já descrito no contexto de ambas as infeções, procedemos à análise dos perfis de citocinas nos soros de ratinhos infetados somente com *Plasmodium*, coinfetados e injetados com lisados anteriormente a uma infeção com *P. berghei*. Nos grupos de ratinhos coinfetados, onde a inibição da infeção hepática de *P. berghei* está presente, era notória uma sobre expressão de MCP-1, MIP-1α e IL-6, sugerindo o seu possível envolvimento.

Uma vez que tanto MCP-1, como MIP-1α são citocinas quimiotáticas para macrófagos e monócitos, o envolvimento destes tipos de células imunitárias na modulação da infeção hepática de *P. berghei* num hospedeiro infetado por *T. brucei* foi avaliado. Primeiramente, realizámos uma depleção de macrófagos em ratinhos infetados somente com *P. berghei* e coinfetados com primeiramente com *T. brucei* e, 5 dias depois, com *P. berghei*. Contudo, não nos foi possível observar uma recuperação de uma infeção normal de *P. berghei* no grupo coinfetados, o que indica que estas células não medeiam esta interação ou que existem mecanismos compensatórios em ação. Assim sendo, e visto que MCP-1 e MIP-1α são citocinas quimiotáticas para monócitos, foi realizada uma nova experiência onde foi bloqueado o recrutamento de monócitos em ratinhos infetados somente com *P. berghei* e coinfetados. Interessantemente, também nestes ratinhos, não se observou uma infeção hepática de *P. berghei* normal, pelo que concluímos que estas células também não estão envolvidas na interação após o bloqueio do recrutamento de monócitos.

Concluindo, esta dissertação demonstra que o sistema imunitário do hospedeiro é um importante mediador da inibição de uma infeção hepática de *Plasmodium*, num hospedeiro previamente infetado com *Trypanosoma*, mais concretamente através da intervenção de citocinas que possivelmente mobilizam células imunitárias que eliminam esporozoítos e EEFs ao longo da infeção de *Plasmodium*, deixando margem para posterior investigação dos mecanismos subjacentes.

PALAVRAS-CHAVE: malária, *Plasmodium*, doença do sono, *Trypanosoma*, coinfecção, sistema imunitário

LIST OF FIGURES AND TABLES

LIST OF ABBREVIATIONS

ACK: Ammonium-chloride-potassium lysis buffer
AIDS: Immunodeficiency syndrome
APC: Antigen presenting cell
BCR: B-cell receptor
BSA: Bovine serum albumin
BSF: *T. brucei* bloodstream form
CCR2: C-C chemokine receptor type 2
CD: Cluster of differentiation
cDNA: Complementary deoxyribonucleic acid
dNTP: Deoxynucleotide triphosphate
DNA: Deoxyribonucleic acid
DNAse: Deoxyribonuclease
DMEM: Dulbecco's Modified Eagle Medium
EEF: *P. berghei* exoerythrocytic forms
eef1a: Elongation factor-1 alpha
FBS: Fetal bovine serum
GFP: Green fluorescent protein
GPI: Glycosylphosphatidylinositol
HAT: Human African trypanosomiasis
HEPES: 4-(2-hydroxyethyl) -1-Piperazineethanesulfonic Acid
HIV: Human immunodeficiency virus
HGF: Hepatocyte growth factor
HMI: Hirumi's Modified Iscove's Medium
Hprt: hypoxanthine guanine phosphoribosyl transferase
HSPG: Heparan sulphate proteoglycans
Huh7: Human hepatoma cell line
IFN-γ: Interferon gamma
IGC: Instituto Gulbenkian da Ciência
IL: Interleukin
ILC: Innate lymphoid cell
iMM JLA: Instituto de Medicina Molecular João Lobo Antunes
i.p: Intraperitoneal
i.v: Intravenous
JHT: Immunoglobulin joining region heavy chain
KC: Kupffer cell
KHB: Krebs-Henseleit buffer
KO / (-/-): Knockout
NEAA: Non-Essential amino acids
NK: Natural killer cell
NKT: Natural killer T cell
NO: Nitric oxide
$PbGFP_{CON}$: Transgenic *P. berghei* ANKA that constitutively expresses GFP
$PbGFP\text{-}LUC_{CON}$: Transgenic *P. berghei* ANKA that constitutively expresses GFP-LUC fusion
PBS: Phosphate-buffered saline
PCF: *T. brucei* procyclic form
PCR: Polymerase chain reaction
Pen-strep: Penicillin-Streptomycin
PFA: Paraformaldehyde
PV: Parasitophorous vacuole
PVM: Parasitophorous vacuole membrane
qRT-PCR: quantitative Real-Time Reverse Transcription-PCR
RAG2: Recombinase activating gene-2
RBC: Red blood cell
RNA: Ribonucleic Acid
ROS: Reactive oxygen species
RPMI: Roswell Park Memorial Institute medium
RT: Reverse transcriptase
SEM: Standard error of the mean
STH: Soil-transmitted helminthiasis
TCR: T-cell receptor
TCRβ: T-cell receptor β-chain
TCRδ: T-cell receptor δ-chain
TLR: Toll-like receptor
TNF-α: Tumor necrosis factor alfa
Treg: Regulatory T lymphocyte
UIS: Upregulated in sporozoite
VSG: Variant surface glycoprotein
WHO: World Health Organization
WT: Wild-Type
$\Delta\Delta C_T$: Comparative C_T
γc: Common cytokine receptor γ chain

TABLE OF CONTENTS

1. INTRODUCTION

1.1 Malaria - Etiology, transmission, symptoms and socio-economic burden

According to the latest World Health Organization (WHO) report, malaria transmission occurs in 91 countries worldwide, 43 of them located in Africa (Figure 1.1)[1]. Consequently, a total of 3.3 billion people are at risk of contracting this disease, leading to as many as 216 million annual cases of malaria, which result in around 445.000 deaths, most of them in children under five years old[1,2].

The infection is caused by intracellular apicomplexan parasites, belonging to the *Plasmodium* genus[3], which infect a large range of vertebrate hosts, including humans[4]. Mammalian infection takes place when, upon blood feeding, an infected female *Anopheles* mosquito inoculates parasites in the host's dermis along with its saliva[5]. There are six *Plasmodium* species known to infect humans: *P. falciparum*, which is responsible for the most severe forms of infection, leading to the highest mortality rates[3]; *P. vivax*, which gives rise to dormant hepatic forms (responsible for relapses) and, along with the former, accounts for the majority of malaria cases[6]; *P. ovale*, also produces dormant forms, nevertheless disease manifestations are usually not severe[4]; *P. malariae*, which is typically silent[7]; *P. knowlesi*, previously thought to only infect macaque monkeys[8]; and *P. simium*, the species most recently identified as capable of infecting humans[9].

Symptoms associated with malaria include metabolic acidosis, severe malarial anemia, cerebral malaria, renal failure, pulmonary edema and jaundice[2]. Consequently, and besides a dramatic death toll, malaria as severe impacts on productivity, reflecting a yearly loss of 12 billion US$ in the Gross Domestic Product (GDP) of affected countries[1]. Despite the worldwide investment and efforts to overcome and prevent the disease, these measures remain insufficient and progress in the fight against malaria has halted.

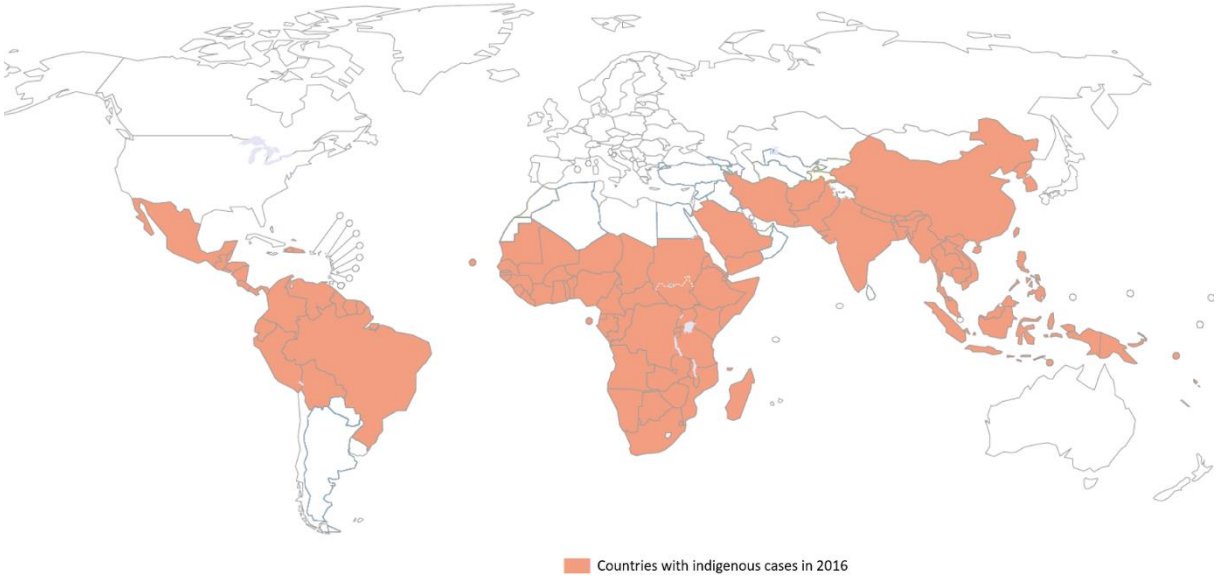

Figure 1.1 – Countries and territories with indigenous cases in 2016. Countries with reported cases of malaria as of 2016 are depicted in orange[1].

1.1.1 *Plasmodium* spp. - life cycle

The life cycle of *Plasmodium* parasites starts when, during a blood meal, an infected female *Anopheles* mosquito inoculates between 15 to 123 salivary gland sporozoites into the host's dermis[10]. Sporozoites then use gliding motility to reach the host's endothelial cells and enter circulation through a cell traversal process[3,11]. These motile forms then home to the liver, where they traverse several hepatocytes until productive invasion of a final hepatocyte occurs, with formation of a parasitophorous vacuole (PV)[10,12]. Once inside the hepatocyte, intra-hepatic parasite forms, also known as

exoerythrocytic forms (EEFs), initiate a process of asymptomatic replication, culminating in thousands of merozoites for each invader sporozoite, a process also known as hepatic schizogony[10,13]. After 2 to 17 days incubation period, depending on the *Plasmodium* and host species[14], these intra-hepatic release vesicles containing thousands of merozoites, called merosomes. These will rupture during pulmonary circulation[5] and discharge the merozoites into the bloodstream that will subsequently invade red blood cells (RBCs). Erythrocytic schizogony ensues, which, depending on *Plasmodium* species, consists of 48 to 72 hours asexual replication cycles, that correspond to the fever periodicity[14]. Each replication cycle results in additional numbers of merozoites, which will then infect new RBCs[5]. During this process, a fraction of the merozoites differentiates into sexual forms[5,10], originating male and female gametocytes that are infective to *Anopheles* mosquitoes, when ingested upon blood feeding from the mammalian host[3]. Inside the mosquito, these gametocytes undergo sexual replication, forming zygotes that mature into motile ookinetes that invade the mosquitoes' midgut, and subsequently develop into oocysts. As oocysts mature, sporozoites are generated within. By the end of the sporozoite development, oocysts burst, allowing sporozoites to migrate to the salivary glands, completing the parasite's life cycle and allowing for the initiation of a new mammalian infection by the invertebrate vector (Figure 1.2)[5,10,15].

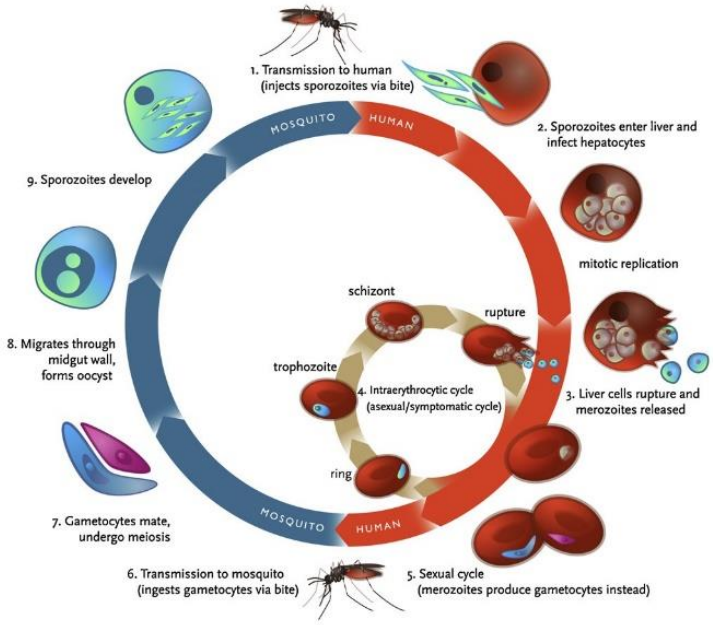

Figure 1.2 ***Plasmodium*** **life cycle**[15]. During the bite of an infected mosquito, sporozoites are injected into the host's skin and home to the liver where they invade hepatocytes. After finishing the development inside these cells, merozoites are released into the bloodstream and infect erythrocytes. Inside, these parasite forms replicate, leading to formation of asexual forms that perpetuate the cycle of infection inside the host and sexual forms, termed gametocytes, that are taken up by uninfected mosquitoes that bite an infected host. Ingested gametocytes undergo sexual replication inside the mosquito midgut, generating sporozoites that migrate to the salivary glands, allowing a new cycle of infection.

- **Liver infection**

The pre-erythrocytic stage of *Plasmodium* infection includes all steps since sporozoite deposition under the skin of the mammalian host until the release of the first merozoites into the bloodstream[3,16]. Hepatocyte infection by the sporozoites is a pivotal step for parasite replication and is conventionally termed the liver or hepatic stage of infection[11]. The liver vasculature is composed by sinusoids with a fenestrated endothelium with protruding highly sulfated heparan sulfate proteoglycans (HSPGs), that can interact with proteins on the surface of the sporozoites, such as the circumsporozoite protein (CSP)[11,17]. Besides, the liver sinusoids are enriched in liver-resident macrophages called Kupffer cells (KCs)[18] through which *Plasmodium* parasites can migrate to gain access to the parenchyma[11,18,19]. A prior study has shown that wildtype (WT) sporozoites wound and traverse KCs while sporozoites incapable of cell traversal remain trapped inside KCs, that degrade them, indicating that cell traversal

possibly aids the parasites resisting phagocytosis by other immune cells[19]. Furthermore, the traversal of KCs may offer advantages due to the shorter time period in which the sporozoites are susceptible to clearance by phagocytic cells[19] and due to the fact that KCs undergo apoptosis after exposure to sporozoites, which might affect mounting of a protective immune response[18,19].

After crossing the sinusoids, sporozoites traverse several hepatocytes inside transient vacuoles, from which they egress, when sensing low pH[20] in the hepatocyte what will become their host cell[12,20]. Upon invasion of the final hepatocyte, sporozoites form a PV with a porous membrane (PVM) derived from the host cell plasma membrane[18,21], which allows entrance of small host factors and nutrients into the vacuole[22]. Sporozoites without this vacuole are rapidly clearly by host cells through apoptosis-dependent mechanisms, which suggests its essential role[23]. The PVM contains several resident proteins, such as upregulated in infectious sporozoites (UIS) 4^3, that may play a role on parasite growth and survival, as evidenced by the deletion mutants of this protein that are unable to develop beyond early liver stages[18].

Upon productive invasion, sporozoites differentiate into active replicative forms called trophozoites[21]. Each of these will enter a process of rapid repetition of closed mitosis, called schizogony, ultimately leading to the formation of several thousand progeny, in the form of a schizont[22]. Eventually, several invaginations of the parasite plasma membrane start packaging individual hepatic merozoites with a single nucleus and necessary organelles[18,22]. These merozoite-filled merosomes bud off from the infected hepatocytes, allowing the release of merozoites into the bloodstream[24].

1.2 Sleeping sickness - Etiology, transmission, symptoms and socio-economic burden

Trypanosoma brucei is a hemoflagellate protozoan that parasitizes various mammalian hosts and is responsible for causing Human African Trypanosomiasis (HAT), also known as sleeping sickness[25], and Animal African Trypanosomiasis (Nagana), which affects cattle[26]. According to the WHO, sleeping sickness is present in 30 African countries and, despite the recent reduction in reported disease cases from 2184 in 2016 to 1447 in 2017, 61 million people, as well as several million heads of cattle, remain at risk of being infected[27,28].

Infection occurs when a vector fly from the *Glossina* genus, also known as Tsetse, injects trypanosomes upon blood feeding on the mammalian host[26]. Humans can be infected by two subspecies of *T. brucei* (Figure 1.3): *T. b. gambiense*, which has humans as its main reservoir, is found in Western and Central Africa and triggers a chronic illness[29]; *T. b. rhodesiense*, whose main reservoir is cattle, is present in Eastern and Southern Africa[30] and causes the most severe and acute form of the disease in humans[29].

Pathology arises in two different clinical stages, the first being the hemolymphatic stage, when parasites invade the circulatory and lymphatic systems, leading to fever, headaches, malaise, muscle and joint pain, anemia, coupled with renal and heart failure[25,26]. As infection progresses, the parasites invade the central nervous system and penetrate through the blood brain barrier[25]. Here, the second or meningo-encephalitic stage takes place and is characterized by the disruption of the sleep-wake pattern, as well as psychotic episodes, convulsions, paralysis and motor disorders similar to those of Parkinson's[29]. Finally, if left untreated, the infection will cause irreversible neuronal damage, leading to coma and, ultimately, death[25,29].

Altogether, this neglected disease represents a major socio-economic concern, due to reduced labour force and diminished livestock production, reflected in a net loss of 4.5 billion US$ annually[28].

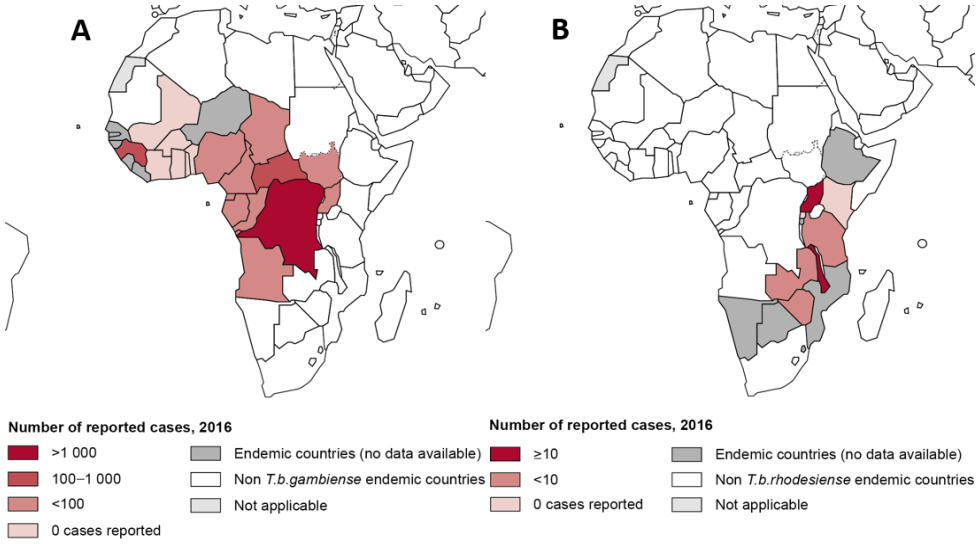

Figure 1.3 – Sleeping sickness geographical distribution, 2016. (A) Endemic countries for *T. b. gambiense*. **(B)** Endemic countries for *T. b. rhodesiense.*[30]

1.2.1 *Trypanosoma brucei* - life cycle

The life cycle of *Trypanosoma brucei* starts when a Tsetse bites a mammalian host upon a blood meal and injects metacyclic forms of trypanosomes together with its saliva[25]. *T. brucei* then invades the bloodstream, the lymphatic system and the changes in the environment induce differentiation into long slender forms which replicate through binary fission, rapidly proliferating and establishing parasitemia[25,31]. During the course of the infection, *T. brucei* parasites can invade the adipose tissue depots, which have been described as a major reservoir for infection, where they differentiate into adipose tissue forms (ATFs) which are transcriptionally different from bloodstream forms (BSFs)[32]. As infection progresses, the escalating parasite density in the blood triggers some parasites to differentiate through a quorum sensing-like mechanism[25]. During the differentiation phase, the highly replicative BSFs develop into non-dividing BSFs, known as stumpy forms, which are able to infect Tsetse flies[25,31]. In case the vector bites an infected host, the stumpy forms will undergo new complex biochemical and morphological changes, giving rise to proliferative procyclic forms (PCF). Finally, *T. brucei*'s life cycle is completed when PCFs reach the Tsetse salivary glands where they develop into quiescent metacyclic forms.

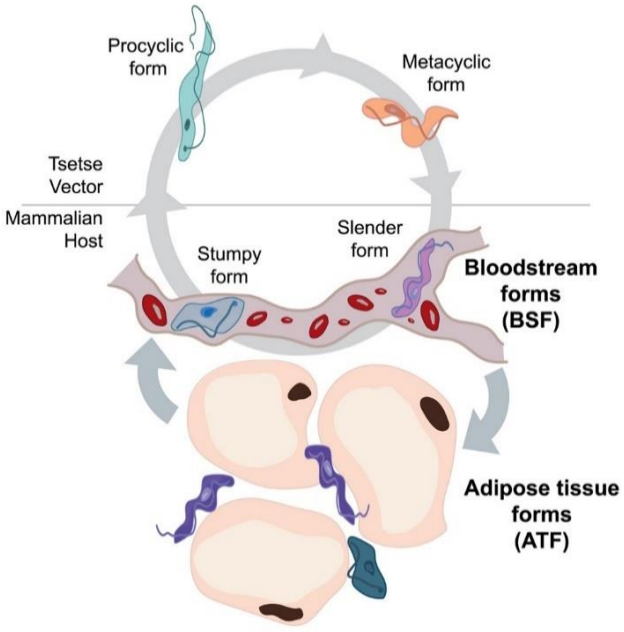

Figure 1.4 - *T. brucei* life cycle.[32] During the life cycle, *T. brucei* alternates between an insect vector, the tsetse fly, and a mammalian host. Different forms of the parasites allow them to proliferate in the vector and in the host (procyclic and slender forms respectively) and to pre-adapt for the transmission (metacyclic forms, in the vector and stumpy forms in the host). Within the mammalian host, parasites can also accumulate and persist in the adipose tissue and are termed adipose tissue forms.

1.3 Immune response against *Plasmodium* spp. liver infection and *Trypanosoma brucei* infection - An overview

The liver is particularly enriched in complex repertoires of immune cells[33,34]. Besides, as only around one hundred hepatocytes are infected by sporozoites upon one infectious bite[35], the liver acts as a bottleneck of infection, representing a potential target for parasite elimination[3,35]. Since the immune system plays a major role in the elimination of *Plasmodium* parasites[10], this section addresses the contribution of myeloid and lymphoid cells in the immune response against *Plasmodium* liver infection, as well as the role of the most notorious cytokines upregulated during this stage.

On the other hand, extracellular parasites are constantly confronted with both humoral and cellular immune responses[36]. For trypanosomes, the exposure to the host's defense mechanisms would easily lead to inevitable elimination if these parasites did not evolve efficient immune escape mechanisms, such as antigenic variation, to hinder an effective immune response[37]. The immunological interplay between *Trypanosoma brucei* and the mammalian host will be addressed below, with particular focus on the contributions of myeloid and lymphoid cells and the most relevant cytokines.

1.3.1 Myeloid cell function

- ***Plasmodium* spp**.

Immune cells from the myeloid cell lineage include monocytes/macrophages, neutrophils, basophils and eosinophils. The possible involvement of basophils and eosinophils during *Plasmodium* hepatic infection remains understudied. Nevertheless, it has been shown that neutrophils and monocytes/macrophages confer the first line of defense against *Plasmodium* liver infection and the host's immune system hinges on these subsets of immune cells to eliminate the parasites[38].

Despite being key mediators of inflammatory response, the role of neutrophils in the context of *Plasmodium* liver infection is poorly addressed[38,39]. Nevertheless, it has been shown that, upon infection, these cells are recruited into the liver sinusoids and induce liver damage by interacting with superoxide dismutases and enhancing the production of reactive oxygen species (ROS), which kill the intra-hepatic parasite forms[39].

The liver is the organ where the largest population of macrophages is found[34]. These cells are known to be highly phagocytic, with an extensive array of surface receptors, such as toll-like receptors (TLRs) and cluster of differentiation (CD) 36 that allow them to interact with diverse classes of organisms[40,41]. Macrophages may display different phenotypes and functions depending on the cytokine environment where they are, which can favor either a pro-inflammatory or anti-inflammatory immune response, leading to an increase of inflammation or tissue repair, respectively[38]. Macrophages not only limit *Plasmodium* liver infection during parasite traversal of these cells, but they can also be activated by parasite factors, such as glycosylphosphatidylinositol (GPI) anchor, leading to the secretion of pro-inflammatory cytokines like interferon-γ (IFN-γ) and tumor necrosis alpha (TNF-α)[40] that eliminate parasites through production of NO[5]. Besides, these immune cells can phagocytose the EEFs, controlling parasite load in the liver[42,43]. Moreover, as being antigen presenting cells (APCs), KCs can also activate T lymphocytes, promoting T cell proliferation and pro-inflammatory cytokine production, which in turn may lead to an adaptive immune response[34,42,44].

- ***Trypanosoma brucei***

The recruitment of immune cells to the site of infection is necessary for an inflammatory immune response against invading pathogens[45]. During a *T. brucei* infection, the exposure to *Trypanosoma*l DNA and the variant surface glycoproteins (VSG) activate monocytes and macrophages[46,47]. Consequently, these cells exert phagocytic activity on the parasites and produce pro-inflammatory cytokines (for instance IFN-γ and TNF-α), as well as trypanotoxic molecules such as nitric oxide (NO)[48,49]. This

inflammatory response is crucial to control parasitemia[50], especially to restrain the first peak of parasitemia, which is fatal in mice depleted of macrophages[51].

Furthermore, although poorly investigated, during the inflammatory immune response to a *T. brucei* infection, neutrophils infiltrate into the liver, leading to hepatic damage and consequent hepatomegaly, a hallmark of a *Trypanosoma* infection[52]. Neutrophils possess pathogen-killing mechanisms that are activated upon a *T. brucei* infection such as phagocytosis[52,53]. Nevertheless, a recent study showed that the overall action of neutrophils in the context of such infection supports parasite establishment, enhancing early *T. brucei* infection onset, although the underlying mechanisms remain to be elucidated[53].

1.3.2 Lymphoid cell function

Lymphoid cells are commonly associated with specific and long-lasting immunity against pathogens, usually referred to as acquired immunity[54]. The cells from the lymphoid lineage can only engage in specific responses upon signaling from the myeloid cells. Naïve T lymphocytes develop in the thymus and mature into effector T cells, which express specific receptors for antigens called T-cell receptors (TCR) and mediate cellular and humoral immunity[16,54]; immature B cells are found in the bone marrow, where they mature into developed B lymphocytes, which express B-cell receptors (BCR) and secrete antibodies[54,55].

- **T cell function**
  - ***Plasmodium* spp.**

T cells play an important role in immune responses and to date, many T cell subsets have been described. Among them are: T helper cells or $CD4^+$ T cells, which express the CD4 surface glycoprotein, express a TCR composed by an alpha and a beta chain (αβ TCR)[56,57]; Cytotoxic T cells or $CD8^+$ T cells, which express the CD8 surface glycoprotein and express the αβ TCR[56,57]; Regulatory T cells (Treg), which differentiate from $CD4^+$ T cells and also express an αβ TCR[54]; Natural killer T cells (NKT), which specifically recognize glycolipid antigens[54]; and γδ T cells, which express an exclusive TCR composed by a γ chain and a δ chain (TCR γδ)[54,57].

T lymphocytes are essential for protective immunity during *Plasmodium* liver infection[16]. $CD4^+$ and $CD8^+$ T lymphocytes have been shown to limit parasite growth through the production of pro-inflammatory cytokines, such as IFN-γ and TNF-α[16,57]. It is described that $CD4^+$ T cells can not only directly inhibit the development of liver stage parasites by production of inflammatory cytokines[57], but also assist in the induction of $CD8^+$ T cell responses when in the presence of a specific T helper (Th) epitope termed P30[57,58]. $CD8^+$ T cells, typically show cytotoxic properties that allow them to eliminate infected hepatocytes through exocytosis of cytotoxic granules that store apoptosis-inducing molecules[16].

On the other hand, the functional contribution of γδ-T lymphocyte in *Plasmodium* liver stage has been the target of several studies[57,59]. Although rather unexplored, the role of these cells in protective immunity against liver stage parasites was shown in murine models lacking αβ T cell receptors[57]. In this study, αβ T cell (-/-) mice that were immunized through the bites of irradiated *Plasmodium*-infected mosquitoes displayed partial protection when challenged with fully infective sporozoites, showing the possible involvement of this T cell population in the elimination of *Plasmodium* sporozoites. Furthermore, upon antibody mediated depletion of γδ-T cells in αβ T-cell-deficient mice, the immune response against sporozoites previously observed was completely abolished, which confirmed the synergistic role of αβ-T and γδ-T cells in the partial protection against *Plasmodium* parasites[57].

  - ***Trypanosoma brucei***

Similarly to their role in a *Plasmodium* infection, $CD4^+$ and $CD8^+$ T lymphocytes are pivotal for the resistance against trypanosomiasis, limiting parasite growth through the production of the pro-inflammatory cytokines IFN-γ and TNF-α[50].

Nonetheless, despite controlling parasite growth, this sustained pro-inflammatory response would be a harmful event for the host. Hence, the intervention of another regulatory T lymphocytes (Treg) is required[60]. Induced expansion of this subset of cells leads to downregulation of IFN-γ, TNF-α and reactive oxygen species (ROS), delaying immunopathology and prolonging the host's survival[60]. The suppression of the inflammatory immune response by production of IL-10 by Tregs and $CD4^+$ T cells restricts extreme inflammatory responses which are unfavorable to both host and parasite by inevitably leading to the death of the host[60].

- **B cell function**
  - ***Plasmodium* spp.**

B lymphocytes are the only cells responsible for the generation of protective antibodies[55]. Although sporozoite-specific B cell memory and cells that generate large amounts of antibodies, termed plasma B cells are poorly studied, studies employing radiation-attenuated sporozoites, as well as genetically modified sporozoites have shown that antibodies can block infection at the pre-erythrocytic stages[55]. This impairment of infection can occur through several mechanisms, including inhibition of sporozoite motility in the dermis or in the liver[5], opsonization of sporozoites and subsequent phagocytosis by macrophages in the spleen and liver[55], blockage of sporozoite invasion into the hepatocytes by preventing the sporozoite ligand to interact with the receptors in the hepatocyte, and inhibition of the parasite's development inside the hepatocytes[5].

  - ***Trypanosoma brucei***

B lymphocytes are quintessential for the control of a *T. brucei* infection due to the continuous interplay between the antibodies produced by this subset of immune cells and the parasite's surface, covered with VSGs. During the early stages of infection, polyclonal B cell activation occurs as a mechanism to cope with parasite proliferation, containing its dissemination[61]. Since the surface of *T. brucei* is entirely coated by VSG, specific antibodies are raised against the epitopes of this protein[62]. As such, these parasites developed an immune evasion mechanism termed antigenic variation. This mechanism is based on a stochastic change to a different VSG type, independently of antibody response[63], by manipulation of VSG gene expression[64]. The host's immune system recognizes that VSG, producing antibodies against it[64]. As parasites expressing this VSG are eliminated, a downwards slope in parasitemia ensues[65]. Simultaneously, some parasites change their expression to a different VSG and are not recognized by the antibodies and proliferate, leading to a new wave of parasitemia, and creating a chronic infection[64,65]. Due to these interactions throughout the infection, B cells play a major role in parasite clearance and control, as displayed in research employing B cell-deficient mice which slowly control the infection for up to 4 weeks, but eventually perish due to the gradually increasing level of parasitemia[63].

1.3.3 Cytokines

Cytokines are small proteins responsible for the communication between cells, mediating immunity and allergic responses[66]. Although numerous and produced by different subsets of cells, such as lymphocytes, monocytes and macrophages, they can be functionally divided into two groups: pro-inflammatory and anti-inflammatory[66].

  - ***Plasmodium* spp.**

IFN-γ is one of the most important pro-inflammatory cytokines during a *Plasmodium* infection[67,68]. The essential role of IFN-γ for the elimination and control of parasite growth has been shown in studies which made use of either antibodies to deplete IFN-γ[67] or IFN-γ-deficient mice[68]. Moreover, this cytokine is able to induce the inducible nitric oxide synthase to produce nitric oxide, which can directly eliminate *Plasmodium* EEFs[5]. Furthermore, upon infection, KCs produce interleukin (IL) 12 and IL-18,

which have been shown to play a synergistic role in controlling infection by further inducing IFN-γ production[69,70].

Contrarily to IFN-γ, whose role in the context of *Plasmodium* infection has long been established, there are cytokines such as tumor necrosis factor α (TNF-α) and IL-6 whose involvement in this process is controversial. In spite of previously contradictory results where TNF-α failed to induce a protective effect, independently of the schedule, dose or murine strain[71], research on the influence of TNF-α and IL-6 in a *Plasmodium* infection reports that these cytokines interact with each other, priming an oxidative burst by generation of ROS that inhibit intra-hepatic parasite development[71,72,73].

- ***Trypanosoma brucei***

IFN-γ has the most significant impact on a *Trypanosoma* infection by eliminating the parasites through production of NO, as shown by studies where IFN-γ-deficient mice infected with *T. brucei* present higher parasitemia peak and shorter survival times than wildtype mice equivalently infected[50]. This cytokine is not only produced by macrophages, because it can activate $CD4^+$ and $CD8^+$ T lymphocytes also lead these cells to further produce it[74,75]. Furthermore, IFN-γ acts synergistically with TNF-α which possesses trypanolytic activity, that leads to elimination of the parasites and control of parasitemia[49,76].

1.4 Coinfections

A coinfection is understood as an infection of the same host by several pathogens, simultaneously[77,78]. In natural populations, coinfection of individual hosts by multiple parasite species is commonly observed[77]. To understand coinfections, two concepts have to be considered: exposure, or the act of the host coming in contact with the pathogen; and susceptibility, which measures the probability of the exposure to the pathogen leading to an infection. A gap in knowledge exists that does not allow discernment between the relative roles of exposure of the hosts and their susceptibility to generate a mixture of parasites and densities within them. Without the ability to perceive the role of each variable, successful medical interventions for coinfected populations become noticeably arduous[79].

Previous studies show that exposure is necessary, but not sufficient for infections, as neither is susceptibility sufficient, in spite of being necessary[80]. Since exposure of hosts to parasites and susceptibility of the hosts are the two core processes that define distributions of infections[79], it is pivotal to comprehend how the geographical distributions of different overlapping infections may lead to coinfected individuals.

Exposure of the host is, at a basic level, a spatial problem[79], although other factors like host behavior play a crucial impact on exposure to parasites[81]. This is well established in classic parasitological examples of infection in humans such as doing chores during the mosquito's peak of activity, which will alter the risk of mosquito bites, which in turn changes exposure to malaria infection[79] and an individual's sexual behavior which affects the risk of multiple sexually transmitted diseases[82]. Furthermore, reports show that parasitic infections causing behavioral changes within the hosts which facilitate parasite transmission is an increasingly common phenomenon[81].

On another hand, susceptibility is not a spatial or behavioral problem, but rather a measure of probability that the exposure of a host to a parasite leads to an established infection[79]. This includes host genetics[83], the host's diet and other factors within the host that may lead to different outcomes of an infection. Reports of the impact of host genetics and diet (occurring both directly and immunologically, through autoimmune diseases) and how these differ on different parasites in different niches are vast leading to the conclusion that there is no optimum host genotype, diet or immune response that provides resistance or tolerance to every infection. Contrarily, susceptibility in coinfections is poorly studied due to the complexity of factors that may alter the outcome of the relation between host and parasites[79]. Two coinfecting species may have antagonistic, synergistic or null effects on each other[84,85,86,87]. These

interactions may occur directly, where a product of one species negatively or positively affects another species inside the host[86], or indirectly via the immune system, such that an immune response triggered by one species can eliminate another (in case of an antagonistic relationship)[87] or provide the niche required for the second species to thrive[88].

1.4.1 Coinfections between *Plasmodium* spp. and other pathogens

The hazards of the concomitant presence of *Plasmodium* parasites and other infectious agents have already been documented[84,88,89]. The outcome of malaria coinfections with either soil-transmitted helminthiasis (STH) or human immunodeficiency virus (HIV) or malaria superinfections will be briefly reviewed below.

The high prevalence of STH in Africa is attributable to two major species of helminths, the *Ascaris lumbricoides* (roundworm) and *Trichuris trichiura* (whipworm). There is evidence that STH deregulates cellular immune responses, downregulating immune responses against *Plasmodium* infection, which may increase susceptibility to infection by the latter without severe symptoms. Moreover, although helminth infections protect against further hemoglobin reduction during acute *P. vivax* malaria, they represent an important risk factor for *P. falciparum* caused anemia[84].

Human immunodeficiency virus (HIV) is a pathogen that preferentially replicates inside $CD4^+$ T lymphocytes. Late stage HIV infections are characterized by an acquired immunodeficiency syndrome (AIDS), which makes the host more susceptible to opportunistic infections. Furthermore, the immune responses triggered during *Plasmodium* infection, where $CD4^+$ T lymphocytes are activated, and pro-inflammatory cytokines are upregulated, offer the ideal environment for HIV replication. For this reason, an exacerbation of AIDS is observed in coinfected individuals [88].

Malaria superinfection is the name given when a host is infected at least twice by *Plasmodium.* There is evidence that if both infections by *Plasmodium* develop normally, hyperparasitemia and swifter death might ensue. However, this might not be the case and, as shown in a rodent model study, an ongoing blood stage infection can inhibit a subsequent liver infection[89]. A possible explanation for this observation is the augmented production of hepcidin, a key regulator of the entry of iron in the circulation of mammals[90], that results in reduction of iron in the hepatocytes, preventing EEF development[89].

As shown in Figures 1.1 and 1.3, *Plasmodium* and *Trypanosoma brucei* parasites are coendemic in numerous African countries, which raises concerns about the possible consequences of coinfections for these population's health and economy[78,91,92]. It has also been reported that *T. brucei* and *Plasmodium* coinfections can occur in areas where both parasites coexist, such as in Sudan and Kenya, where 42% and 100% of sleeping sickness patients, also suffer from malaria[91,92]. Interactions between these parasites have recently been studied, and research has shown that a simultaneous infection with *T. brucei* and *P. berghei* blood stage parasites result in higher parasitemias, stronger anemias and reduced survival in coinfected mice[78]. However, barely any effort has been made either to uncover the mechanisms behind these results nor the possible outcomes of a coinfection between trypanosomes and *P. berghei* liver stages.

1.5 Experimental models for Malaria and Sleeping Sickness

Liver stage malaria research makes use of several hepatic cell lines, which are easy to maintain and replicate in the laboratory and have a well-defined genome, being permissive to genetic manipulation[3]. As of late, a great variety of experimental *in vivo* models are available to accomplish these studies, allowing researchers to investigate parasite-host interactions from a whole organism point of view[3,93], since these models allow the development of high throughput drug therapy assays, vaccination therapies and a comprehensive study of the cell biology of the liver stage[94]. It is also possible to genetically modify both mice and parasites, simulating specific experimental conditions[13]. Although several experimental

parasite models are used at iMM JLA's Prudêncio Lab, *P. berghei***,** which naturally infects rodents and does not pose a health threat to humans[3], stands above the others. C57BL/6J mice present higher susceptibility to hepatic infection to *P. berghei* than other mouse strains[95], making it a preferable system to study the biology and immunology of liver stage parasites[96].

In sleeping sickness, mice are used as "model hosts", because they are not considered "natural hosts" for trypanosomes[93]. *T. b. brucei* is typically used at IMM-JLA's Figueiredo Lab given that it is a highly proliferative non-human infective variant of *T. b. rhodesiense*, which also shares genetic similarities with *T. b. gambiense*[93]. The C57BL/6J mice also feature a higher resistance and survivability when challenged with a *T. b. brucei* infection[97], showing promise as the main experimental model.

2. PRELIMINARY RESULTS

The Prudêncio and Figueiredo Labs have established a *T. brucei/P. berghei* coinfection protocol to evaluate the outcome of an ongoing *T. brucei* infection in a subsequent *P. berghei* infection (Figure 2.1). The experimental group (coinfected group) was first infected with *T. brucei* (day 0) and 5 days later (peak of *T. brucei* parasitemia) *P. berghei* sporozoites were also injected. The other group was single infected with *P. berghei*, simultaneously with the coinfected group.

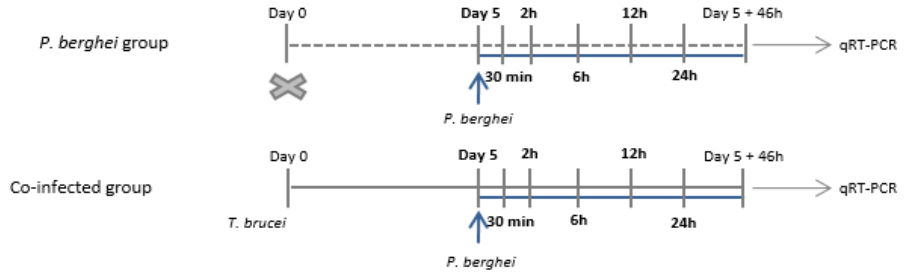

Figure 2.1 - Schematic representation of the coinfection protocol. Mice are either infected with *P. berghei* only, acting as a control for liver infection (*P. berghei*, top) or infected with *T. brucei* at day 0, and five days later injected with *P. berghei* sporozoites (Coinfected, bottom). Livers were collected at different timepoints of *P. berghei* liver infection; before parasite replication (30 min, 2h, 6h, 12h), during parasite replication (24h) and before merozoite release into the bloodstream (46h).

In order to evaluate the impact of an ongoing *T. brucei* infection on a subsequent *P. berghei* liver infection, mouse livers were collected at several time-points post-sporozoite injection, as shown in Figure 2.1. The mice were sacrificed and *P. berghei* liver load was assessed through qRT-PCR at several timepoints during *P. berghei* infection: between 30 mins and 12 hours of infection, where replication of intra-hepatic *P. berghei* has not yet been initiated; at 24 hours, where *P. berghei* replication is ongoing; and 46 hours, which corresponds to a late stage of *P. berghei* liver development, but when merozoites have not yet been released into the bloodstream[98].

A dramatic impairment of *P. berghei* liver infection was observed as a result of a primary *T. brucei* infection, as seen in Figure 2.2. Moreover, the decrease in *P. berghei* infection could be observed as early as 30 min post-sporozoite injection, suggesting that a rapid elimination of *P. berghei* may take place while sporozoites are homing to the liver or immediately after hepatocyte invasion.

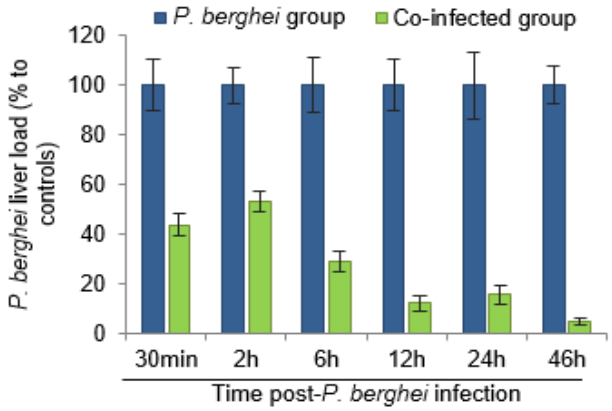

Figure 2.2 – Effect of *T. brucei* ongoing infection on a subsequent infection by *P. berghei*. *P. berghei* liver load quantification 30 min, 2, 6, 12, 24 and 46 hours post-sporozoite infection in naïve mice (blue bars) or 5 days post *T. brucei* infection (green bars). Results are expressed in means and error bars represent standard error of the mean

The total *P. berghei* liver load results from the quantification of the genes encoding *P. berghei* 18S rRNA therefore, the reduction observed in *P. berghei* liver infection could be due to either a decrease in the number of EEFs and/or a decrease in the size of each EEF. To distinguish between these possibilities,

an immunofluorescence microscopy analysis of infected liver sections was performed, which showed a lower number of infected hepatocytes as early as 6 hours post-sporozoite injection (Figure 2.3A). To complement these results, confocal microscopy enabled the measurement of *P. berghei* EEF areas, revealing a normal development of *P. berghei* parasites that successfully invaded liver cells (Figure

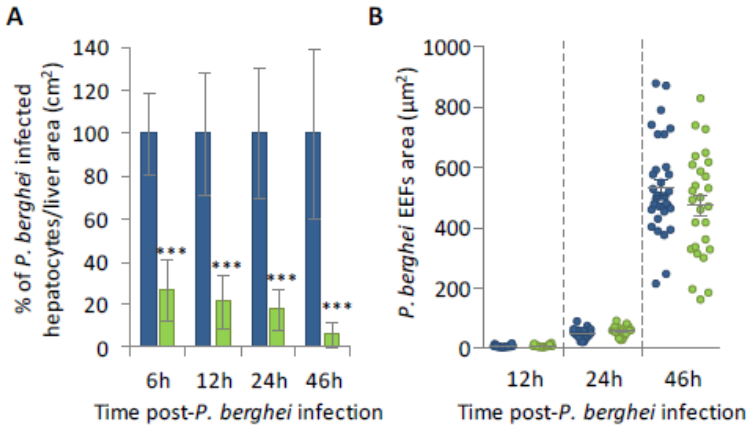

Figure 2.3 - Effect of *T. brucei* infection on the number of *P. berghei* EEFs (A) *P. berghei* EEFs microscopical quantification 6 h, 12 h ,24 h and 46 hours after sporozoite injection in naïve mice (controls – blue bars) or mice infected with *T. brucei* 5 days prior to *P. berghei* infection (coinfected – green bars). **(B)** *P. berghei* EEFs size measurements by confocal microscopy 12 h, 24 h and 46 hours after sporozoite injection in naïve mice (controls – blue dots) or mice infected with *T. brucei* 5 days prior to *P. berghei* infection (coinfected – green dots). Results are expressed in means and error bars represent standard error of the mean.

2.3B) of mice previously infected by *T. brucei*.

Interestingly, the impairment of *P. berghei* liver stage infection by *T. brucei* could be phenocopied by the injection of *T. brucei* lysates. Injection of *T. brucei* lysates into naïve mice 30 minutes prior to injection of *P. berghei* sporozoites resulted in a dose dependent impairment of *P. berghei* liver infection, suggesting that effect is mediated by (a) *T. brucei* molecule(s) (Figure 2.4).

In spite of the the array of preliminary data already obtained, the mechanism by which an ongoing *T. brucei* infection leads to impairment of *P. berghei* hepatic infection remains unestablished. Since the immune system plays a major role during coinfections[79], the host labs' research was directed to investigating the immune responses triggered by *T. brucei*, and their possible impact on *P. berghei* liver infection.

Immunodeficient murine models are frequently used due to their extensive applications in different fields such as human hematopoietic stem cells studies, parasitic infections and cancer research[99]. To assess the involvement of the immune system in the *T. brucei*/*P. berghei* coinfection phenotype, the host labs made use of a C57Bl6/J mouse model with gene knockouts ((-/-)) in the recombinase activating gene-2 (RAG2) and in the common cytokine receptor γ chain (γc). Consequently, mice with the RAG2^{-}

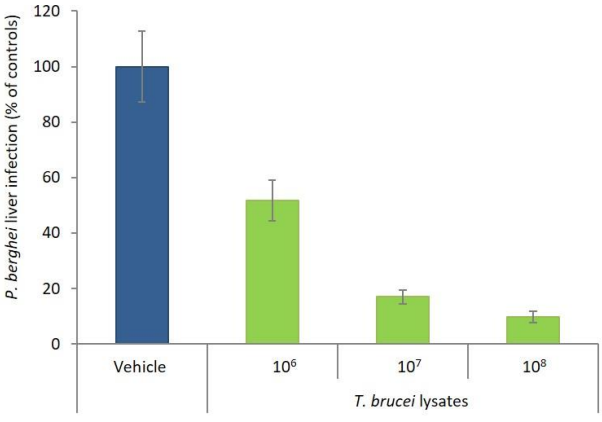

Figure 2.4 – Dose-de ... *P. berghei* liver load quantification at 46 hc ...ected with three differ- ent concentrations of ... Results are expressed in means and error bar...

$^{-/-}/\gamma c^{-/-}$ double mutations are completely alymphoid and lack T and B lymphocytes, natural killer cells (NK) and innate lymphoid cells (ILC)[99].

P. berghei liver infection was assessed in either wildtype and RAG2$^{-/-}/\gamma c^{-/-}$ mice which were infected only with *P. berghei* or coinfected (first with *T. brucei* and 5 days later with *P. berghei*). In order to assess the involvement of these cells not only in the invasion impairment, but also in the subsequent decrease on the number of EEFs, livers were collected at 6 and 46 hours post-*P. berghei* infection. The results obtained showed that RAG2$^{-/-}/\gamma c^{-/-}$ mice present a normal *P. berghei* liver infection at the 6 hours post-sporozoite injection, but only a partial recovery at 46 h post-*P. berghei* infection, when previously infected with *T. brucei* (Figure 2.5), suggesting that immune lymphoid cells are involved in the impairment of *P. berghei* hepatocyte invasion by *T. brucei*.

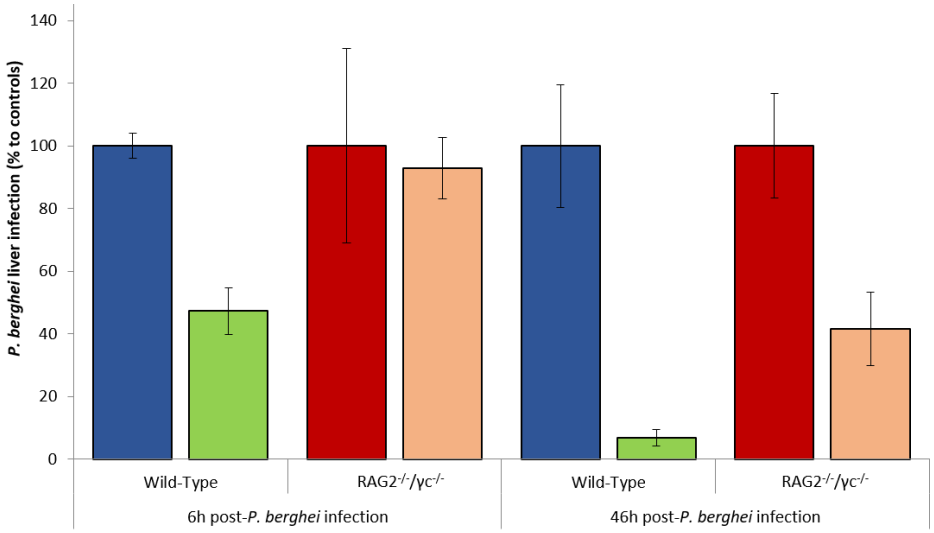

Figure 2.5 – Effect of an ongoing *T. brucei* infection on *P. berghei* liver infection in wildtype and RAG2$^{-/-}/\gamma c^{-/-}$ mice. *P. berghei* liver load quantification at 6 and 46 hours post-sporozoite injection in wildtype naïve mice (blue bars) or mice infected 5 days beforehand with *T. brucei* (green bars) and RAG2$^{-/-}/\gamma c^{-/-}$ naïve mice (red bars) or mice infected 5 days beforehand with *T. brucei* (orange bars). Results are expressed in means and error bars represent standard error of the mean.

To further elucidate which lymphoid cells may be taking part in the elimination of *P. berghei* parasites in coinfected hosts, a C57Bl6/J model with a mutation in RAG2 was employed. These mice differ from those previously used due to the fact that they only lack T and B lymphocytes[100]. Four groups of mice were sacrificed at 6 h and 46 hours: one group of RAG2$^{-/-}$ mice single infected with *P. berghei*; one group of RAG2$^{-/-}$ mice infected by *T. brucei* 5 days prior to *P. berghei* infection; and two groups of wildtype mice equivalently infected, as controls. Similarly to the previous observations, data evidenced a recovery of a normal *P. berghei* infection in RAG2$^{-/-}$ coinfected mice at 6 hours (Figure 2.6). This suggests that either T cell, B cells, NKT cell or γδ T cells play a role in the impairment of *P. berghei* hepatic infection by an ongoing *T. brucei* infection.

Nevertheless, albeit pivotal for clearance of parasites in the early stages of *P. berghei* infection, neither of these subsets of immune cells have an impact on the *Trypanosoma*-mediated impairment of *P. berghei* infection at the 46 hours timepoint (Figure 2.6).

In conclusion, available data demonstrates that *T. brucei* and its lysates impair a subsequent infection by *P. berghei* by preventing sporozoite invasion of the hepatocytes and by elimination of EEFs. Furthermore, it is possible to conclude that the host's immune system plays a pivotal role mediating this interaction, although the underlying mechanism remains to be elucidated.

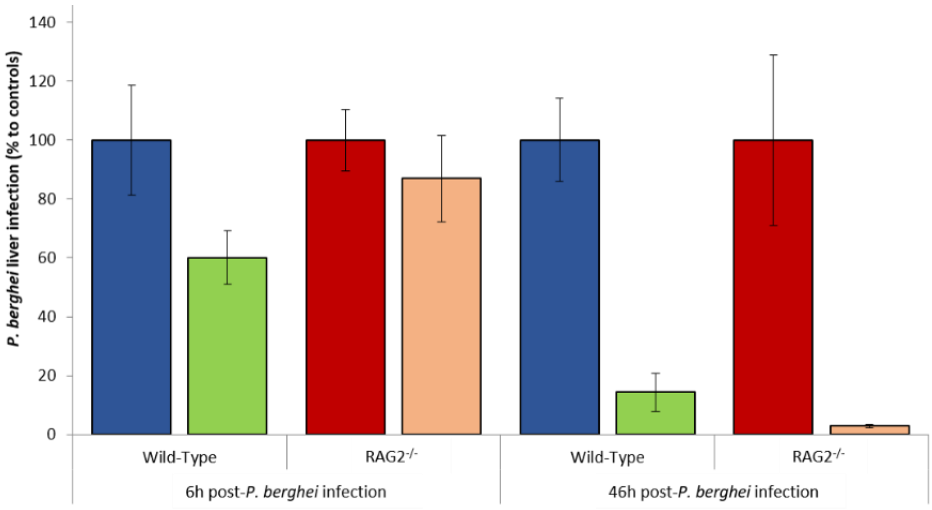

Figure 2.6 – Effect of an ongoing *T. brucei* infection on *P. berghei* liver infection in wildtype and RAG2$^{-/-}$ mice. *P. berghei* liver load quantification at 6 and 46 hours post-sporozoite injection in wildtype naïve mice (blue bars) or mice infected 5 days beforehand with *T. brucei* (green bars) and RAG2$^{-/-}$ naïve mice (red bars) or mice infected 5 days beforehand with *T. brucei* (orange bars). Results are expressed in means and error bars represent standard error of the mean.

3. OBJECTIVES

Host lab observations have shown that both an ongoing *T. brucei* infection and the injection of *T. brucei* lysates impair a subsequent *P. berghei* liver infection. Furthermore, the available data indicate the observed decrease in *P. berghei* liver infection likely occurs through two independent mechanisms, one of which acts during invasion of the host hepatocytes and another that mediates the elimination of intra-hepatic parasites. However, each of these mechanisms remains to be elucidated. The objective of the present work is to shed light on the possible involvement of immune responses on the mechanisms by which either an ongoing *T. brucei* infection or pre-administration of *T. brucei* lysates impair *P. berghei* hepatic infection. To accomplish this, we propose to:

(i) implement an *in vitro* system that will simulate host environmental cues triggered by *T. brucei* that mediate the impairment of *P. berghei* hepatic infection;

(ii) unravel the contribution of specific immune cells and factors in the mechanism by which *T. brucei* infection impairs hepatocyte invasion by *P. berghei*;

(iii) evaluate the duration of the protection conferred by *T. brucei* lysates against *P. berghei* liver infection;

(iv) assess cytokine profiles at different timepoints following either a coinfection with *T. brucei* and *P. berghei* or injection of *T. brucei* lysates and subsequent *P. berghei* infection;

(v) correlate the cytokine profiles and the differential extent of inhibition of *P. berghei* liver infection obtained in (iv) in order to select and assess the involvement of specific immune cells on the impairment of *P. berghei* liver infection.

4. MATERIALS AND METHODS

Mice

Both *in vivo* and *ex vivo* experiments were performed using C57Bl/6J mice, from Charles River Laboratories. T-cell receptor β-chain deficient mice (TCRβ (-/-)) and mice deficient for the heavy chain joining region of immunoglobulins (JHT (-/-)) were obtained from Instituto Gulbenkian da Ciência (IGC). T-cell receptor δ-chain deficient mice (TCRδ (-/-)) and mice deficient in Interferon-γ production (IFNγ (-/-)) were kindly provided by Bruno Silva-Santos laboratory, Instituto de Medicina Molecular João Lobo Antunes (iMM JLA). Experimental mice used for *in vivo* experiments were 7 to 10 weeks old, while for *ex vivo* purposes they were 10 to 27 weeks old. Mice were housed in specific pathogen-free conditions, at the Rodent Facility at iMM JLA. All the experimental work was performed according to the EU regulations and was approved by ORBEA (AWB_2015_09_MP_Malaria).

Parasite Lines

Trypanosoma brucei

Trypanosoma brucei brucei AnTat 1.1 90:13 pleomorphic and *Trypanosoma brucei brucei* 427 wild-type monomorphic strains were used in this study. AnTat 1.1 90:13 is a transgenic parasite line that constitutively expresses EP1 (glu-pro repeat-containing) surface proteins, tetracycline repressor and T7 RNA polymerase[101]. Both parasite strains were cryo-preserved in HMI-11 culture medium (HMI-9 medium[102] without serum plus) with 7% glycerol (10^6 trypanosomes/mL in 200 uL) and stored at -80°C. *T. brucei* bloodstream forms were cultured at 37°C in 5% CO_2 in HMI-11 medium, where parasite density was maintained below $1x10^6$ trypanosomes/mL for the pleomorphic strain and $2x10^6$ trypanosomes/mL for the monomorphic strain.

Plasmodium berghei

This study employed *Plasmodium berghei* ANKA line 259cl2 expressing Green Fluorescent Protein (GFP) ($PbGFP_{CON}$, mutant RMgm-5)[103] and *Plasmodium berghei* ANKA line 676m1cl1 expressing a GFP-firefly luciferase protein fusion ($PbGFP\text{-}LUC_{CON}$, mutant RMgm-29)[104], where each transgene is constitutively expressed under the control of elongation factor-1 alpha (eef1a) promoter throughout the parasite's life cycle.

Hepatocellular human carcinoma cell line culture

Adherent Huh7 human hepatoma cells (10.000 per well) were cultured in 96-well plates at 37°C in 5% CO_2 in Roswell Park Memorial Institute medium (RPMI 1640, GIBCO) and supplemented with 1% (v/v) HEPES buffer (GIBCO), 1% (v/v) Sodium Pyruvate (GIBCO), 1% (v/v) Penicillin-Streptomycin (Pen-Strep, GIBCO), 1% (v/v) L-Glutamine (GIBCO), 1% (v/v) Non-Essential Amino Acids (NEAA, GIBCO) and 10% (v/v) heat-inactivated Fetal Bovine Serum (FBS, GIBCO). Cells were always used between passages 3 and 12, after thawing from -80°C storage.

Mouse liver slices

For mouse liver slice cultures, a modified version of an established protocol was employed[105]. Briefly, mice were euthanized by isoflurane inhalation and 200 U.I. of heparin in 200 µL of phosphate buffered saline (PBS 1x) were administered by intravenous (i.v.) injection. Livers were perfused through the portal vein by flushing 10 mL of ice-cold oxygenated Krebs-Henseleit Buffer (KHB, described below) using a peristaltic pump at a speed of 16 mL/min. The heart's right atrium was sniped to allow out-flow. Livers were dissected, and one lobe was embedded in a 5 % (w/v) low melting temperature agarose and allowed to cool until solid. This lobe was sectioned in slices ranging from 100 µm to 300 µm, using a Vibratome® Series 1500 – Tissue Sectioning System (Technical Products International).

Agarose was removed with a blade and the slices were kept in ice-cold KHB until transferred to a culture plate pre-warmed to 37ºC, filled with Dulbecco's Modified Eagle Medium (DMEM, GIBCO), supplemented with 1 % (v/v) L-Glutamine, 10 % (v/v) FBS, 4,5 g/L D-Glucose (GIBCO), 5 % (v/v) Pen-Strep, 1 % (v/v) fungizone (GIBCO), 10 mM of HEPES buffer, 1 % (v/v) NEAA, 20 mM of Sodium Pyruvate and 50 µg/mL of ascorbic acid (Sigma). The liver slices were incubated at 37°C in 5% CO_2 and medium was replaced every 24 hours.

Krebs-Henseleit Buffer

One litre of a 10x concentrated KHB stock solution was prepared by combining two solutions. The first was obtained by dissolving 3,67g of $CaCL_2 \cdot 2H_2O$ (Sigma) in 500 mL of ultrapure water. The second required dissolution of 3,73g of KCl (Sigma), 69g of NaCl (Sigma), 2,71g of $MgSO_4 \cdot 7H_2O$ (Sigma) and 1,63g of KH_2PO_4 (Sigma) in 500 mL of ultrapure water. After mixture of both solutions, the 10x concentrated KHB stock solution was filtered through a 0,22 µm filter and stored at 4°C.

On the day of the liver collection, 500 mL of 1x concentrated KHB were prepared by diluting 50 mL of 10x KHB in 250 mL of ultrapure water at 4ºC and by adding a pre-prepared solution composed of 1.05g of $NaHCO_3$ (Sigma), 2,475g of D-Glucose Monohydrate (Sigma), 1.19g of HEPES (Roth) in 200 mL of ultrapure water.

The 1x KHB was kept at 0-4ºC in melting ice and was oxygenated with 95% O_2 for 30 min.

Hematoxylin and Eosin staining

At 30 min, 1 hour, 24 hours and 48 hours post liver collection, liver slices were fixed in 4% paraformaldehyde solution (PFA), washed in PBS 1x and embedded in paraffin. Four µM sections obtained using the microtome Leica RM2145 were placed in slides and immersed in a primary xylol solution (Klinipath) for 10 min, followed by a second immersion in xylol for 5 min. For the first step of the staining, slides were washed following a gradient of ethanol solutions: 100% ethanol for 5 min, 95% ethanol for 5 min and 70% ethanol for 5 min; after which the slides were washed with distilled water for 5 min. Subsequently, slides were stained with Harris's Hematoxylin (Bio-Optica) for 3 min and washed with running water for 5min. For the second step of the staining, slides were immersed once in 70% ethanol and then four times in eosin (Shandom-Thermo), followed by a 30 sec sequence of washes using the aforementioned ethanol gradient, but starting from the lowest to highest ethanol concentration. Finally, slides were immersed in xylol for 10 min and mounted with a lamella with xylol solution and observed under brightfield light using NanoZoomer SQ (Hamamatsu) after drying.

In vivo* injection of live *T. brucei

Mice were infected with 2.000 *T. brucei* AnTat 1.1 90:13 parasites/100 µL through intraperitoneal (i.p.) injection[32]. All the parasites came from a vial stored at -80°C, which was thawed. The number of motile parasites was counted in a Neubauer chamber and parasites were diluted in HMI-11 medium.

***T. brucei* lysates preparation**

T. brucei 427 wild-type monomorphic strain cultures were expanded, as described above, in order to have the desired amount of parasites. Trypanosomes were harvested by centrifugation at 3000 g for 15 min at 4°C. The supernatants were discarded, and the parasite pellets were pooled and centrifuged as in the previous step. The supernatant was again discarded, and the trypanosome pellet was resuspended in either PBS 1x (for *in vivo* experiments) or RPMI culture medium (for *in vitro* experiments). The parasite suspension was kept on ice and the parasites were mechanically disrupted by sonication, using a Soniprep 150 (MSE), using a sonication sequence of 6 cycles of 1 min 30 sec sonication at maximum intensity and 30 sec pauses. Parasite lysis was verified by microscopy using a Olympus CKX31 inverted microscope, after which aliquots of the fresh lysates were flash frozen in liquid nitrogen and stored at -80°C.

In vivo injection of *T. brucei* lysates

For *in vivo* purposes, mice were injected with lysates of 10^8 trypanosomes/200 µL through tail vein i.v. injection. Regarding *in vitro* experiments, huh7 cells were inoculated with 10^6, 10^7 or 10^8 *T. brucei* 427 wild-type parasites lysates in 10 µL.

Infection by *P. berghei*

In vivo

P. berghei sporozoites were obtained from laboratory-reared *Anopheles stephensi* mosquitoes, infected by feeding on infected mice. On day 20-30 after mosquito infection, sporozoites were extracted from mosquitoes' salivary glands by hand dissection and collected into non-supplemented RPMI medium[106]. To obtain free sporozoites, the suspension was mechanically homogenized and filtered through a 40 µm strainer. Sporozoites were counted and the concentration was adjusted to have 30.000 sporozoites/200 µL by adding non-supplemented RPMI medium. Mice were infected with the sporozoite suspension by retroorbital i.v. injection under isoflurane anaesthesia[107].

In vitro

Sporozoites were obtained as described above. Huh7 cells were infected with 10.000 luciferase-expressing *P. berghei* sporozoites[3] in different conditions: RPMI medium with the same supplements used for Huh7 culture; RPMI medium without FBS but supplemented with 10% of fresh heat inactivated serum collected from either *T. brucei*-infected mice or from naïve mice; and 10% of *T. brucei* lysates in RPMI medium, at concentrations mentioned previously. These experimental conditions were also combined with different amounts of splenocytes from either *T. brucei*-infected mice or from naïve mice (50.000, 100.000 or 200.000 splenocytes per well). All medium compositions contained fungizone (1:300) and gentamycin (1:1000). Huh7 cells were incubated for 2 hours at 37°C in 5% CO_2 with each condition and then infected with *P. berghei* sporozoites, followed by a centrifugation of 5 min at 3000 rpm. Finally, cells were incubated for 48 hours at 37ºC in 5% CO_2.

Serum separation

Two experimental groups of mice, one naïve and one infected with *T. brucei*, were used to obtain the serum for either *in vitro* studies or cytokine quantification assays. Blood was collected and allowed to coagulate for 1 hour at room temperature. Serum was separated from blood cells by centrifugation (15 min, 3000g). For *in vitro* experiments, serum was used immediately after collection, while for the cytokine quantification assays it was frozen and stored at -20°C until use.

Cytokine and chemokine quantification

Cytokine quantification assay was performed by Quansys Biosciences, using a chemiluminescent ELISA-based assay (Q-Plex, Screen (16-Plex)). Serum samples obtained as described above were tested for IL-1α, IL-1β, IL-2, IL-3, IL-4, IL-5, IL-6, IL-10, IL-12p70, IL-17, IFNγ, TNFα and GM-CSF cytokines and MIP-1α, MCP-1 and RANTES chemokines. The intensity of the chemiluminescence from each array was measured using Q-view imager (Quansys Biosciences), converted into pg/mL and analysed using Q-View software (Quansys Biosciences).

Isolation of mouse splenocytes

Spleens were collected into a petri dish containing 5 mL of sterile 2% FBS in PBS 1x (FACS buffer), and mechanically homogenized by passing the organ through a 70 µm cell strainer. The cell strainer was washed with 5 mL of FACS buffer and the homogenate was collected into a 50 mL tube. FACS buffer was added to the tube to achieve a final volume of 30 mL, followed by a centrifugation at 1400 rpm, for 8 min at 6ºC. The supernatant was then discarded, and the pellet was resuspended in 3 mL of

Ammonium-Chloride-Potassium (ACK) lysis buffer (1L H_2O, 0,01 mM EDTA, 10 mM $KHCO_3$, 150 mM NH_4Cl) for 3 min at room temperature to lyse red blood cells (RBCs). To stop the lysis reaction, 13 mL of FACS buffer were added and the cell suspension was centrifuged at 1400 rpm for 8 min at 6 ºC. The supernatant was again discarded, and the pellet was resuspended in 13.5 mL FACS buffer. The cell suspension was transferred to a fresh tube through a 40 µm cell strainer, to remove dead cell clumps. Cells were centrifuged again, the supernatant was discarded, and the cell pellet was resuspended in 3 mL of RPMI medium. Cells were then counted in a Neubauer chamber. To exclude dead cells from the counting, an aliquot from the cell suspension was incubated with trypan blue (1:40) prior to loading.

Quantification of gene expression in the liver by quantitative Real-Time Reverse Transcription-Polymerase Chain Reaction (qRT-PCR)

Livers were collected upon euthanasia, and one lobe was snap frozen in liquid nitrogen and stored at -80°C. 0.8-1 mg of each liver was mechanically homogenized in Trizol reagent (Thermofisher) and RNA was extracted following the manufacturer's instructions. RNA was quantified using a NanoDrop 2000 Spectrophotometer. cDNA synthesis was performed using 10 µg of RNA plus NZYtech's reverse transcriptase (RT), as well as random hexamer primers, buffer, RT inhibitor and deoxynucleotide triphosphate (dNTP) solution mix, following the manufacturer's recommendations, for a final reaction volume of 20 µL. Four µL of cDNA were amplified by qRT-PCR using an Applied Biosystems StepOne Plus equipment, in which each 10 µL reaction contained 1x SYBR Green PCR Master Mix (Applied Biosystems) and 0.5µM of each primer (Table 1). The amplification program consisted of a holding stage (95°C, 10 min), followed by 50 amplification cycles (95°C, 15sec and 60°C, 1min). The primers were designed to span exon-exon junctions, to avoid genomic DNA amplification, and so RNA-DNAse treatment was not required. Amplification specificity was verified by melting curve analysis and controls lacking either RT or RNA were also performed to exclude contaminations with genomic DNA or nucleic acids present in the water, respectively (data not shown). Gene expression was analysed by comparative C_T method ($\Delta\Delta C_T$) and each gene was normalized to an endogenous mouse reference housekeeping gene, hypoxanthine guanine phosphoribosyl transferase (*Hprt*).

Table 1 - Sequences of primers used for qRT-PCR.

Target gene	Primers	
	Forward	Reverse
CLEC4f	TGAGTGGAATAAAGAGCCTCCC	TCATAGTCCCTAAGCCTCTGGA
CD68	AGCTGCCTGACAAGGGACACT	AGGAGGACCAGGCCAATGAT
F4/80	CCCAGCTTATGCCACCTGCA	TCCAGGCCCTGGAACATTGG
HPRT	TTTGCTGACCTGCTGGATTAC	CAAGACATTCTTTCCAGTTAAAGTTG
P. berghei 18S rRNA	AAGCATTAAATAAAGCGAATACA TCCTTAC	GGAGATTGGTTTTGACGTTTATGTG

Quantification of *P. berghei* hepatic infection by immunofluorescence microscopy

Livers were collected at euthanasia, and one lobe was fixed in 4% PFA. Twenty-four hours later, the PFA was discarded and the liver lobes were washed and stored in PBS 1x at 4ºC. Fifty µm thick liver sections were prepared using the Vibratome® Series 1500 – Tissue Sectioning System (Technical Products International) and incubated in permeabilization/blocking solution (2% (w/v) Bovine Serum

Albumin (BSA, Fisher Scientific), 0.5% (v/v) Triton-X100 (Roth) in PBS 1x) at room temperature for 1 h, followed by an overnight incubation at 4°C with an α-UIS4 antibody (1:300) (goat, home-made), which targets the *P. berghei* parasitophorous vacuole membrane[108]. Liver slices were washed two times for 5 min with blocking solution, followed by a single wash for 5 min in PBS 1x. Samples were then incubated for 2h at room temperature with the secondary antibody Alexa-Fluor 488 (1:300) (donkey α-goat IgG, Invitrogen™) and with Hoescht 33342 (1:1000) (Invitrogen™) which stains DNA. After two washes with blocking solution and one wash with PBS 1x, 5 min each, slices were mounted on microscope slides using Fluoromount-G™ (SouthernBiotech) and analysed under a widefield fluorescence microscope Zeiss Axiovert 200M. Infection was quantified by determination of the number of the EEFs and normalized to the area of the liver slice. EEF areas were measured using ImageJ software[3]. Representative images were acquired using a Zeiss LSM 710 confocal microscope.

PbGFP-LUC$_{CON}$ *in vitro* infection assessment by bioluminescence

Forty-eight hours after infection of Huh7 cells with luciferase-expressing *P. berghei* sporozoites, cell confluency was assessed by incubation with AlamarBlue® (Invitrogen ™), for 1h at 37ºC, as per the manufacturer's instructions. Fluorescence was measured using an Infinite M200 (Tecan) microplate reader, using and excitation wavelength of 530±9 nm and a detected emission wavelength of 590±20nm. Subsequently, *P. berghei* infection was quantified by measuring luciferase activity, using Firefly Luciferase Assay Kit (Biotium) following the manufacturer's instructions. Briefly, cells were incubated in 70 µL of lysis buffer (1:5 in milliQ H_2O) for 25 minutes in a VWR rocking platform at 600 rpm at room temperature, followed by a 5 min centrifugation at 3000 rpm, to allow all cell debris to deposit. Thirty µL of the resulting supernatant were collected into a 96-well white plate and 50 µL of D-Luciferin (Biotium) were added to each well[3]. Luminescence intensity was immediately measured in relative luminescence units using an Infinite M200 (Tecan) microplate reader.

Macrophage and Monocyte depletion

To deplete macrophages, experimental mice were injected i.v. with liposome-encapsulated clodronate (1 mg/mouse) (clodronateliposomes.org). Control mice were injected with the same volume of PBS filled liposomes (clodronateliposomes.org). The treatment was performed 48 hours prior to *P. berghei* infection.

Regarding monocyte depletion, mice were injected i.p. with α-CCR2 antibody (20 µg/mouse) which targets C-C chemokine receptor type 2 (CCR2)[109] and was kindly provided by Matthias Mack, University Hospital Regensburg. Control mice were injected with the same volume of PBS 1x. This treatment was performed at 48 and 24 hours prior to *P. berghei* infection, upon *P. berghei* infection, and 24 hours post *P. berghei* infection.

Isolation of liver leukocytes

Mouse livers were collected at 46h post *P. berghei* infection into a solution of PBS 1x containing DNAse (2U/mL), mechanically homogenized by passing the organ through a 100 µm filter, followed by a 5 min centrifugation at 2000rpm. The pellet was resuspended in 10 mL of 35% percoll solution (Sigma) in non-supplemented RPMI and centrifuged at 1360g for 20 min without break at 20ºC. The resulting pellet composed of liver leukocytes and RBCs was resuspended in 3mL of ACK lysis buffer to remove RBCs and this reaction was stopped using 7 mL of FACS buffer. After a final centrifugation of 5 min at 2000 rpm, the leukocytes were resuspended in PBS 1x.

Confirmation of monocyte depletion by flow cytometry

After isolation, one million leukocytes from each mouse were plated in 96-well plates and centrifuged at 2000 rpm for 3 min at 4ºC. All traces of liquid were removed, and cells were incubated

in α-CD16/CD32 (eBioscience) for 20 min at 4 ºC. For the staining of myeloid surface antigens, cells were incubated for 20 min at 4 ºC with a mixture of the following conjugated flow cytometry antibodies: FITC-CD11b (Biolegend) (1:400), eF605-Ly6C (Biolegend) (1:400), BV785-MHC II (Biolegend) (1:2000), PE-Cy7-Ly6G (Biolegend) (1:200), e780-FVD (Biosciences) (1:100), PE-CD11c (Biosciences) (1:300)[48]. Finally, cells were resuspended in 25 µL FACS buffer and kept protected from light, at 4ºC, until acquisition. All samples were run on a BD LSRFortessa X-20 with FACSDiva 6.2 software and collected data was analysed using FlowJo software (version 10.4.2).

Statistical analyses

Results were expressed in terms of mean ± standard error of the mean (SEM). Statistical comparisons were made using Student's t-test and Mann-Whitney non-parametric test on GraphPad Prism 7.0. Cytokine expression analysis made use of a hierarchical clustering algorithm based in the Euclidean distance metric and complete linkage method, whose combination allows measurement of the absolute distance between the most dissimilar elements of the clusters[110]. This hierarchical clustering was performed using Cluster (version 3.0), whose results allowed the construction of a heatmap employing Java TreeView software.

5. RESULTS AND DISCUSSION

As previously shown, an ongoing *T. brucei* infection, as well as its lysates impact *P. berghei* liver infection. In order to assess the outcome of *P. berghei* liver infection and the involvement of the host's immune system in this interplay, mice deficient for the production of several immune cell subsets and factors were either injected with *T. brucei* or *T. brucei* lysates and subsequently infected with *P. berghei*.

In this thesis, we attempted to establish an *in vitro* system that would simulate the impairment of *P. berghei* liver infection by *T. brucei* observed *in vivo* (Section 5.1). We then investigated the role of the host's immune system in the impairment of hepatocyte invasion by *P. berghei* in the context of the coinfection model (Section 5.2). Subsequently, we assessed the duration of the inhibitory effect of *T. brucei* lysates (Section 5.3) and evaluated cytokine profiles at several timepoints of *P. berghei* infection following coinfection or administration of *T. brucei* lysates prior to *P. berghei* infection (Section 5.4). Lastly, we assessed the mechanism of *Trypanosoma*-induced impairment of *Plasmodium* liver infection, based on the cytokine profiles obtained in the previous section (Section 5.5).

5.1. Establishment of an *in vitro* system that replicates the impairment of *P. berghei* hepatic infection by *T. brucei*

5.1.1. Improvement of an established *in vitro* system by addition of immune cells

The implementation of an *in vitro* system in the context of a *T. brucei/P. berghei* coinfection by the host labs has not been successful so far (data not shown). However, the previously tested conditions did not include immune cells. Considering that these cells were later found to be involved in the *T. brucei*-mediated impairment of *P. berghei* hepatic infection (Figures 2.5 and 2.6), we hypothesized that the inclusion of immune system components in the previously tested *in vitro* system might contribute to the successful establishment of this system.

In previous experiments, Huh7 cells were incubated in medium containing 10% serum collected from *T. brucei*-infected mice, prior to infection of these cells with *P. berghei* sporozoites, but no impairment in *P. berghei* hepatic infection was observed. We hypothesized that we were unable to replicate a coinfection phenotype *in vitro* due to the absence of immune cells in this system. To overcome this, mouse splenocytes, which mainly consist on lymphocytes, macrophages and dendritic cells, were isolated and added to Huh7 hepatoma cells. After a 2 hour incubation period at 37°C in 5% CO_2, Huh7 cells were infected with luciferase-expressing *P. berghei* sporozoites. Forty-eight hours later, Huh7 confluency was assessed using the Alamar blue metabolic assay, followed by quantification of *P. berghei* infection by bioluminescence.

To test if the inclusion of immune system components is pivotal for the establishment of a successful *in vitro* system, Huh7 cells were infected with sporozoites following incubation under different medium conditions: RPMI medium; RPMI with 10^5 splenocytes either from a naïve mouse or from a mouse infected with *T. brucei* for 5 days; RPMI medium without FBS, but supplemented with 10% of heat inactivated serum either from a naïve mouse or from a mouse infected with *T. brucei* for 5 days; RPMI medium without FBS, but supplemented with 10% of heat-inactivated serum from a naïve mouse and also 10^5 splenocytes isolated either from a naïve mouse or from a mouse infected with *T. brucei* for 5 days; RPMI medium without FBS, but supplemented with 10% of heat-inactivated serum from a mouse infected for 5 days with *T. brucei* and 10^5 splenocytes isolated either from a naïve mouse or from a mouse infected with *T. brucei* for 5 days. The RPMI medium infection was considered as a control for all the conditions, so both confluency and luminescence values were set to 100% for this experimental condition.

If our hypothesis was correct, the readout of the successful establishment of the *in vitro* system would be the observation of a decrease in *P. berghei* hepatic load, when Huh7 cells are incubated with *T. brucei* serum and mouse splenocytes prior to sporozoite addition.

We observed that RPMI supplemented with serum either from a naïve mouse or from a *T. brucei*-infected mouse, there was a reduction in *P. berghei* infection to 42% and 39%, respectively ($p<0,001$ for both conditions), when compared with RPMI not supplemented with serum from mice (Figure 5.1). This result showed that serum itself has an impact on infection, regardless if the host is infected with *T. brucei* or naïve, confirming results obtained previously by the host lab.

The presence of splenocytes from either naïve or *T. brucei*-infected mice partially impaired *P. berghei* infection (74% and 69% of the control, respectively) ($p<0,01$ for both), which reveals that the impairment observed is independent from the status of the host from which the splenocytes were obtained (Figure 5.1). Moreover, serum and splenocytes seem to have a cumulative effect in the impairment of *P. berghei* hepatic infection, as observed in conditions where *P. berghei* infection occurred in the presence of serum from naïve mice and splenocytes either from naïve or mice infected with *T. brucei* (18%, 17%, respectively) (Figure 5.1). An equal result was observed when serum of *T. brucei*-infected mice was combined with splenocytes either from naïve or mice infected with *T. brucei* (18%, 17%, respectively) (Figure 5.1). As such, when added to Huh7 cells, neither serum nor splenocytes from *T. brucei*-infected mice led to a result different from that obtained with their naïve counterparts, which led us to conclude that the impairment of *P. berghei* hepatic infection observed does not result from the involvement of immune system components.

Altogether, this data shows that to reproduce the impairment of *P. berghei* infection by *T. brucei in vitro*, the addition of immune components directly to the cells is insufficient and, as such, a more complex immune environment might have to be simulated for the successful establishment of a *in vitro* model for the coinfection between *T. brucei* and *P. berghei*.

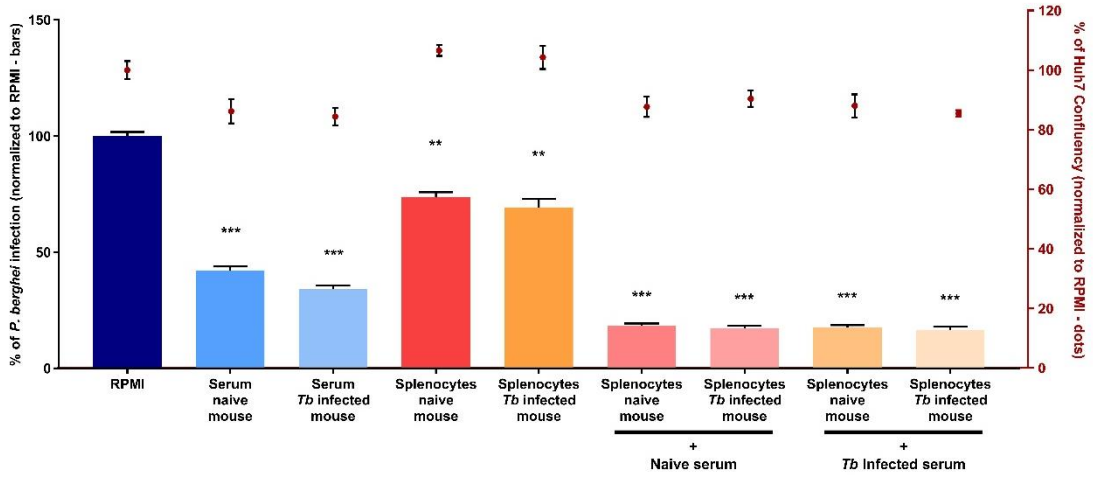

Figure 5.1 – Serum from *T. brucei* infected mice does not impair *P. berghei* hepatic infection, even when combined with splenocytes. Bars: Luciferase quantification of *P. berghei* infection 48 hours post-sporozoite inoculation in Huh7 cells. *Tb*: *T. brucei*. **Dots:** Alamar blue fluorescence measurements for cell confluency. Results are expressed in means and error bars represent SEM. Mann-Whitney test between control and remaining conditions: **p<0,01; ***p<0,001.

In the *in vitro* setup evaluated serum either from naïve or *T. brucei*-infected mice led to an impairment of *P. berghei* infection. We though that it could be probably due to the presence of components that inhibit sporozoites infection, thus we attempted to simulate the impairment phenotype through the use of *T. brucei* lysates. To this end, Huh7 cells were infected with sporozoites after a 2 hour incubation under the following conditions: RPMI medium; RPMI with lysates of 10^7 trypanosomes; RPMI with lysates of 10^6 trypanosomes combined with 10^5 splenocytes from naïve mice; RPMI with lysates of 10^8 trypanosomes combined with 10^5 splenocytes from naïve mice; and RPMI with lysates of 10^7 trypanosomes combined with amounts of splenocytes from naïve mice ranging from $5x10^4$ to $2x10^6$. Two additional conditions were tested, one with flash frozen RPMI medium and another combining flash frozen RPMI medium and 10^5 splenocytes, as a control for the impact of frozen medium on *P.*

berghei hepatic infection, since *T. brucei* lysates are flash frozen. As in the previous experiments, RPMI medium infection was considered as a control for the remaining conditions and confluency and luminescence values were set to 100% for this experimental condition. For our hypothesis to be confirmed, we would expect a decrease in *P. berghei* hepatic load when cells are incubated with *T. brucei* lysates together with naïve mouse splenocytes.

We found that flash frozen RPMI medium had an impact on the outcome of the infection, reducing parasite load to 63% ($p<0,001$), equivalent to the effect observed by lysates of 10^7 trypanosomes. We also observed that a higher concentration of *T. brucei* lysates did not promote a reduction of *P. berghei* infection stronger than the one by frozen RPMI. Even combined with 10^5 splenocytes, *T. brucei* lysates did not show a stronger impairment of *P. berghei* infection than that of frozen RPMI: 49% of a normal *P. berghei* infection for frozen RPMI; 52% of a normal infection for lysates of 10^7 trypanosomes; and 66% of a normal infection for lysates of 10^8 trypanosomes (Figure 5.2A). Furthermore, different splenocyte amounts combined with lysates of 10^7 trypanosomes revealed a *P. berghei* infection between 34% to 69%, similar to those of the conditions incubated only with splenocytes (31% to 69%) (Figure 5.2B).

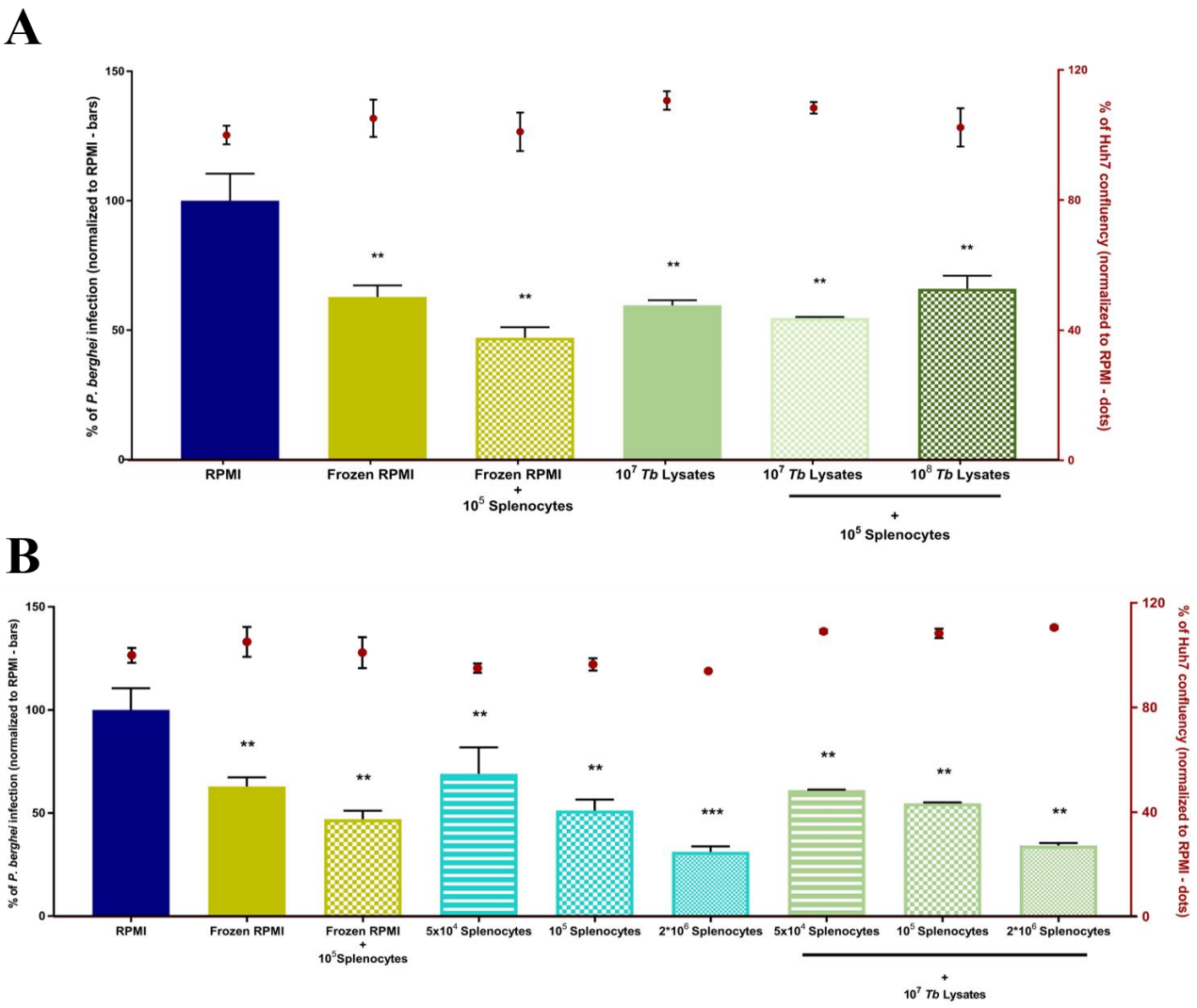

Figure 5.2 – *T. brucei* lysates combined with splenocytes do not impair *P. berghei* hepatic infection. (A) Splenocytes combined with different concentrations of *T. brucei* lysates **(B)** *T. brucei* lysates combined with several concentrations of splenocytes **Bars:** Luciferase quantification of *P. berghei* infection 48 hours post-sporozoite inoculation in Huh7 cells. *Tb* stands for *T. brucei*. **Dots:** Alamar blue fluorescence measurements for cell confluency. Results are expressed in means and error bars represent SEM. Mann-Whitney test between control and remaining conditions: **p<0,01; ***p<0,001.

Overall, our data revealed that *T. brucei* lysates do not impair *P. berghei* infection more than the splenocytes alone. Therefore, we conclude that the combination of *T. brucei* lysates with immune system components is not sufficient to replicate the impairment of *P. berghei* hepatic infection *in vitro*.

5.1.2. Mouse liver slice-based *in vitro* model

The attempt to improve the *in vitro* model for the replication of the phenotype of a coinfection between *T. brucei* and *P. berghei* proved unsuccessful. Therefore, we speculated that the interaction between the splenocytes and the hepatocytes might not be sufficient to reproduce the mechanism by which *T. brucei* impairs *P. berghei* liver infection. To overcome this, we attempted to implement a novel *in vitro* model for *P. berghei* hepatic infection, which relied on the use of mouse liver slice cultures. These cultures retain the original liver tissue structure with all its resident cell types, which include hepatocytes, endothelial and Kupffer cells[111], allowing for the reproduction of possible interactions between these cells *in vitro*, which are absent from the previously used *in vitro* systems for *P. berghei* infection.

Mouse liver slices of 200 µm thickness were incubated in supplemented DMEM and collected at several time points (0h, 1h, 24h, 48h and 72h) to evaluate their survival rate. To this end, three independent methods were employed: the Alamar blue metabolic assay; the load and quality of extracted RNA; and histological analysis. Huh7 cell cultures grown for 24 hours were considered as the positive control for the survival evaluation and, as such, Alamar blue fluorescence values were set to 100% for this experimental condition. To account for background fluorescence, wells containing only Alamar blue diluted in RPMI were also analysed.

Through the Alamar blue assay, we observed that even though all slices were viable at the 0 hours timepoint, a swift decrease in survivability ensues, resulting in presumable death of all slices (Figure 5.3). Nevertheless, slice number 1 had a decay pattern different from the others, that could be explained for its difference in thickness.

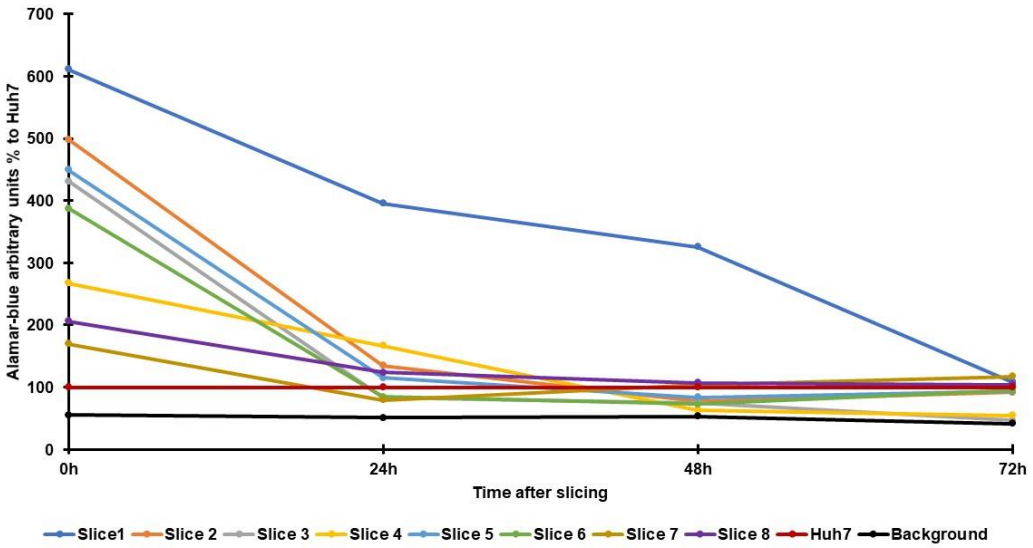

Figure 5.3 – Mouse liver slices show a loss of viability from 24 hours onwards. Alamar blue fluorescence measurements for cell proliferation and viability.

Given that after cell death, RNA degrades very rapidly, we performed a gel electrophoresis of total RNA. In living cells, two distinct bands can be observed, the 4,8kb and 1,8kb bands which correspond to 28S and 18S ribosomal RNA, respectively. RNA extraction from liver slices collected at 0 and 1 hours showed both rRNAs, which translate into undamaged RNA, and therefore viable slices (Figure 5.5). However, from 1 to 24 hours onwards we observed a 21-fold decrease in the amount of total RNA

(Figure 5.4), due to its degradation as shown by the loss of rRNA bands (Figure 5.5), which suggests tissue death.

Timepoint	RNA concentration
0h	879,1 ng/µl
1h	869,5 ng/µl
24h	40,9 ng/µl
48h	41,3 ng/µl
72h	5,9 ng/µl

Figure 5.4 – RNA degradation drastically increases at later timepoints. RNA concentration plunges 1 hour post liver slicing, corroborating Alamar blue assay results.

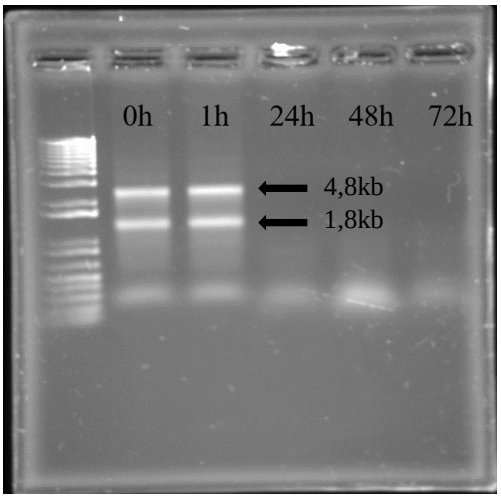

Figure 5.5 – RNA gel electrophoresis reveals 28S and 18S at early but not late timepoints. 4,8kb and 1,8kb bands correspond to 28S and 18S rRNA respectively.

We further confirmed that liver slice death occurred between 1 and 24 hours post sectioning through histological analysis. It was employed an hematoxylin and eosin staining which allows for the detection of cell damage. The results showed that in later timepoints from 24 hours onwards, it could be found in the tissue sections: swollen hepatocytes, which indicates damage or death; apoptotic cells, with their characteristic disappearing nucleae; pyknosis, which is the term given to condensation of chromatin in

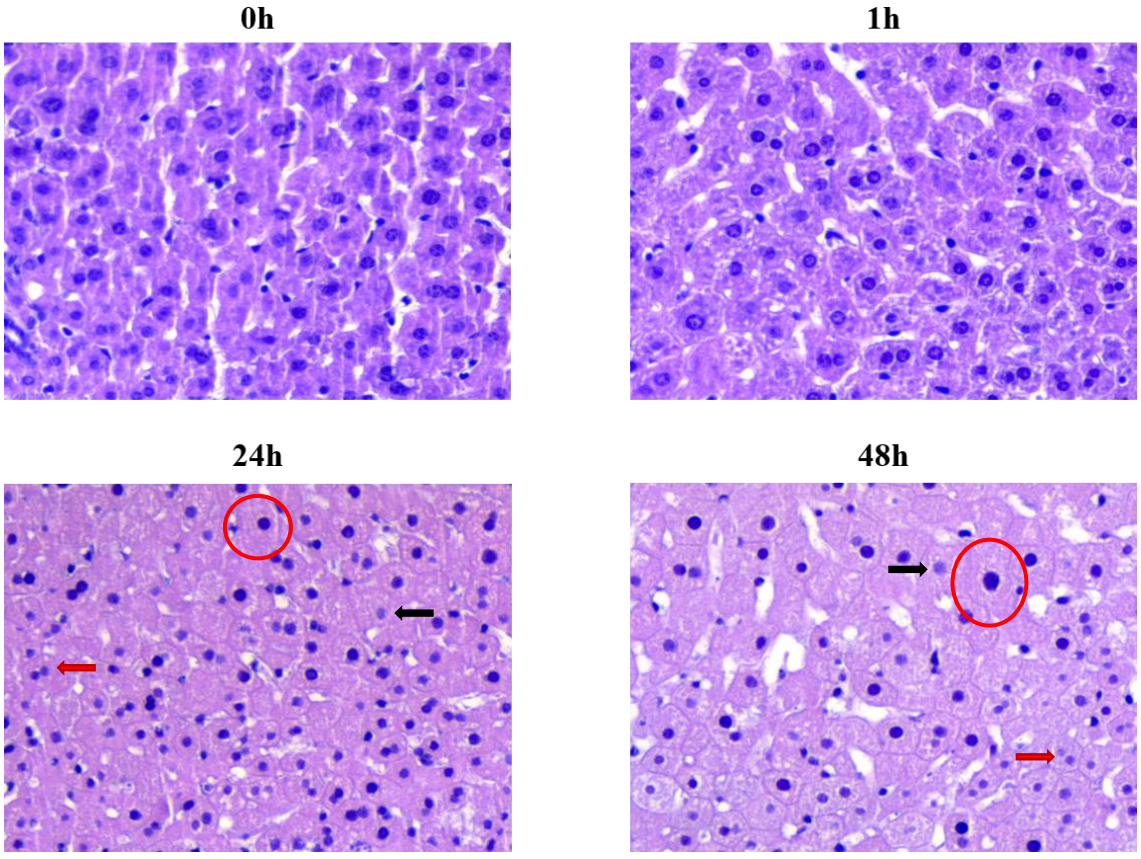

Figure 5.6 – Liver slices evidence clear signs of hepatocyte damage and death 1 hour post slicing. Red circles display swollen hepatocytes; Black arrows indicate apoptotic cells; Red arrows reveal pyknosis examples.

apoptotic cells; and a lighter staining on the cytoplasm of hepatocytes, which is a marker for loss of proteic activity (Figure 5.6).

As shown in Figure 5.3, liver slice 1 exhibited a different pattern of viability decay, when compared with the others. We hypothesize that this could be due to a difference in thickness and that this variable could be determinant for the outcome of survivability. To test this, liver slice thicknesses higher than 200 µm were chosen for better reproducibility of the slices and due to a higher thickness present in liver slice 1, and so livers were cut into 200 µm, 250 µm and 300 µm sections and survivability parameters were assessed at 0h, 24h, 48h and 60h post slicing, through Alamar blue assay and quantification of total RNA.

Huh7 fluorescence values were used as controls and set at 100%, as previously stated. The Alamar blue results revealed a similar pattern of viability decay in all the samples, independently from the liver slice thickness, where it was observed a decrease in fluorescence at 24 hours post slicing (Figure 5.7).

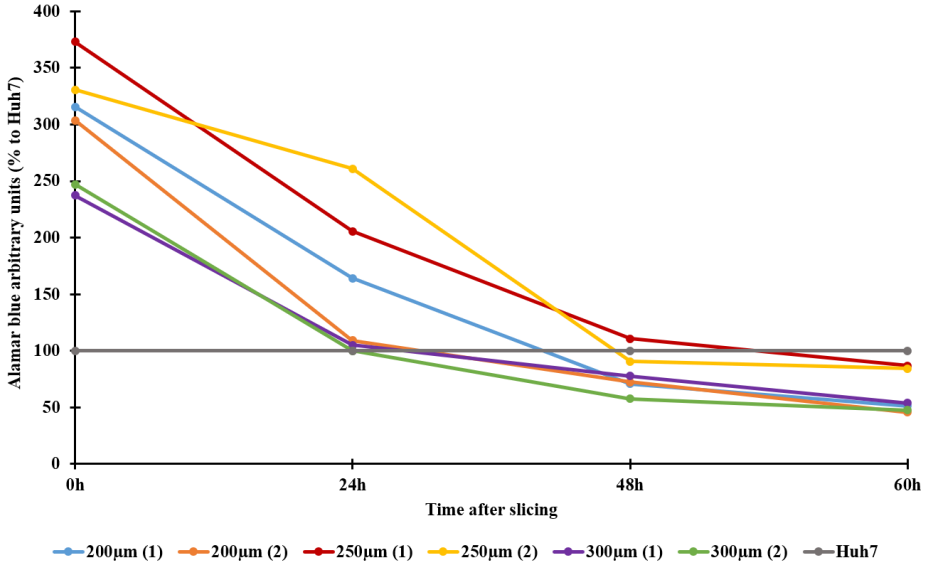

Figure 5.7 – Liver slice loss of viability from 24h onwards is independent of the its thickness. Alamar blue fluorescence measurements for cell proliferation and viability.

Furthermore, RNA quantification results were also consistent with the previous result, confirming that an increase in liver slice thickness does not prolong tissue viability (Figure 5.8).

Timepoint	RNA concentration		
	200 µm	250 µm	300 µm
0h	882,8 ng/µl	1210,1 ng/µl	1319,4 ng/µl
24h	79,7 ng/µl	218,3 ng/µl	97,2 ng/µl
48h	25,3 ng/µl	220,2 ng/µl	120,2 ng/µl
60h	21,5 ng/µl	179,7 ng/µl	130,7 ng/µl

Figure 5.8 – RNA degradation pattern is similar between slices with different thickness. RNA concentration decreases 5 to 13-fold in the first 24 hours post liver slicing.

Overall, the data obtained showed that viable liver slice cultures could not be maintained for longer than 1 hour. Thus, the implementation of a novel *in vitro* model for *P. berghei* hepatic infection relying on this methodology was not successful.

5.2. Mechanism of *T. brucei* infection-induced impairment of hepatocyte invasion by *Plasmodium*

Previous results from the host lab showed that mice lacking either T and B cells play a major role on the immune mechanism by which an ongoing *T. brucei* infection impairs hepatocyte invasion by *P. berghei* (Figure 2.6). As previously stated, since these subsets of cells have an impact on infections of both parasites, we hypothesize that an ongoing *T. brucei* infection activates subsets of these immune cells, which will inhibit *P. berghei* sporozoite invasion. In the following section, we describe our attempts to corroborate our hypothesis.

- **Immune cells – T cell subsets**

To test if T cells were responsible for the *T. brucei*-mediated impairment of hepatocyte invasion by *P. berghei*, we started by taking advantage of mice that lack T-cell receptor β-chain (TCRβ (-/-). Two groups of TCRβ (-/-) mice were used: one infected only with *P. berghei* and another coinfected (primarily infected by *T. brucei* and, 5 days later, by *P. berghei*). In parallel, two groups of wildtype mice were equivalently infected, and all four groups were sacrificed 6 hours post-sporozoite injection and *P. berghei* liver load was assessed by qRT-PCR. If our hypothesis was proven correct, we should observe at least a partial recovery of liver stage phenotype at the 6 hours timepoint of infection in TCRβ (-/-) coinfected mice.

Contrary to our expectations, in TCRβ (-/-) coinfected mice, we observed an impairment of *P. berghei* liver infection, similar to that of wildtype coinfected mice (30% in wildtype and 41% in TCRβ (-/-); $p<0,05$ for both groups when compared with the respective controls) (Figure 5.9), suggesting that T cells were not mediating this impairment. Nevertheless, we cannot exclude an involvement of NKT and γδ T cells, since these T cell subsets are not present in TCRβ (-/-) mice[56].

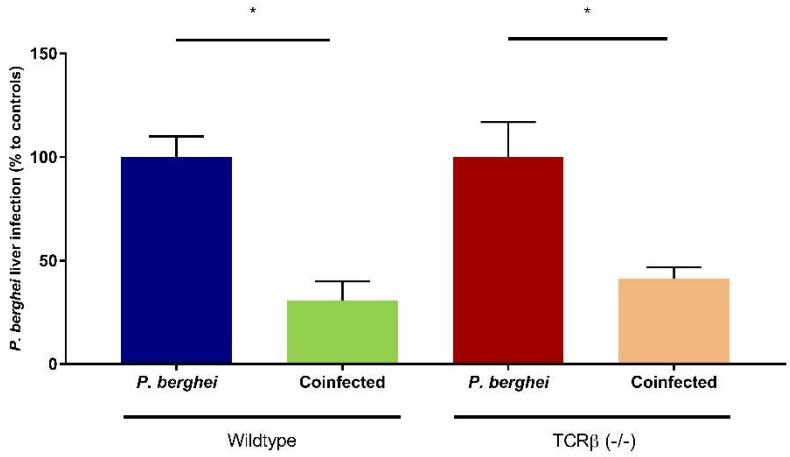

Figure 5.9 – T cells alone are not responsible for the inhibition of *P. berghei* hepatic invasion. *P. berghei* liver load quantification 6 hours post-sporozoite injection in naïve mice (controls: WT – blue; TCRβ (-/-) – red) or mice infected 5 days beforehand with *T. brucei* (coinfected: WT – green; TCRβ (-/-) – orange). Results are expressed in means and error bars represent standard error of the mean. Mann-Whitney test between control and coinfected groups: *$p<0,05$ (n=5 mice per group).

Since the involvement of NKT cells in the *T. brucei*-induced impairment of *P. berghei* hepatic invasion had been previously excluded[51], γδ T cells were the obvious candidates among T cell subsets left to study. Thus, we hypothesize that these cells might be mediating the impairment of *P. berghei* hepatocyte invasion by an ongoing *T. brucei* infection. To assess the role of these cells in the interplay between *T. brucei* and *P. berghei* coinfection, two groups of T-cell receptor δ-chain deficient (TCRδ (-/-)) mice, one single infected with *P. berghei* and another coinfected (primarily infected by *T. brucei* and, 5 days later, by *P. berghei*) were sacrificed at 6 hours post-sporozoite injection and liver load was quantified by qRT-PCR. As controls for *P. berghei* infection and coinfection between *T. brucei* and *P.*

berghei, two groups of wildtype mice were also infected. For our hypothesis to be confirmed, we expected the recovery of a normal *P. berghei* infection in TCRδ (-/-) coinfected mice.

Interestingly, no significant difference was found between TCRδ (-/-) mice and wildtype coinfected mice (49% and 33% of *P. berghei* liver infection, respectively; p>0,05, not shown) (Figure 5.10).

Since we were unable to rescue a normal *P. berghei* liver infection in coinfected mice lacking αβ-T cells and γδ-T cells, we concluded that each of the T cell subsets evaluated is not, by itself, involved in the mechanism of *T. brucei* impairment of hepatocyte invasion by *P. berghei*.

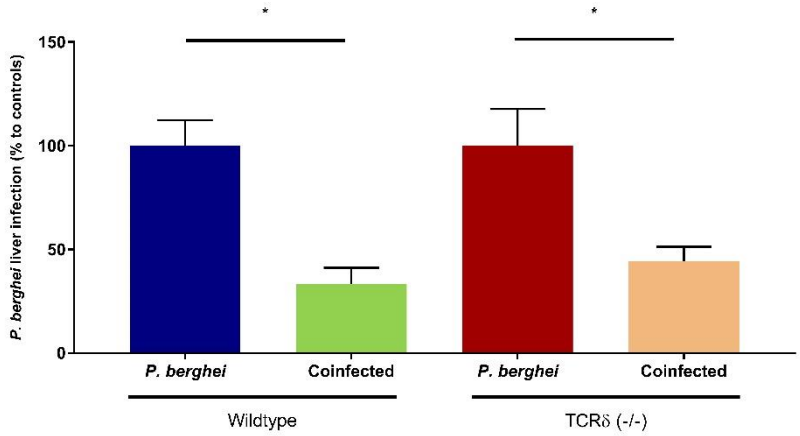

Figure 5.10 – γδ T cells cells singlehandedly do not play a role in the impairment of *P. berghei* hepatic invasion. *P. berghei* liver load quantification 6 hours post-sporozoite injection in naïve mice (controls: WT – blue; TCRδ (-/-) – red) or mice infected 5 days beforehand with *T. brucei* (coinfected: WT – green; TCRδ (-/-) – orange). Results are expressed in means and error bars represent standard error of the mean. Mann-Whitney test between control and coinfected groups: *p<0,05 (n=5 mice per group).

- **Immune cells – B cell activation**

P. berghei liver infection was not rescued in mice lacking T cells. Therefore, we hypothesized that B cells might be playing a role in the *T. brucei*-mediated impairment of *P. berghei* hepatocyte invasion. To test this, we employed mice deficient for the heavy chain joining region of immunoglobulins (JHT (-/-)), which consequently lack B cells. The coinfection model used was the same as that employed in the previous experiment: two groups of JHT (-/-) mice, one infected only with *P. berghei* and another coinfected (primarily infected by *T. brucei* and, 5 days later, by *P. berghei*) and two wildtype groups with equivalent infections. We hypothesized that if this subset of cells was the responsible for the impairment of hepatocyte invasion by *P. berghei* in the coinfected mice, then we should obtain at least a partial recovery of the liver stage impairment phenotype. *P. berghei* liver load quantification at 6 hours showed that in coinfected JHT (-/-) mice, shows a tendency for the impairment of *P. berghei* hepatocyte invasion (33% in wildtype coinfected mice and 65% in JHT (-/-) coinfected mice; p<0,05) (Figure 5.11). Hence, our hypothesis was not confirmed, leading us to conclude that the impairment of hepatic invasion by *P. berghei* during *T. brucei* infection is not mediated by B cells.

Altogether, we were unable to uncover the role of a single cell subset in the *T. brucei*-induced impairment of *P. berghei* hepatic invasion. Nevertheless, we hypothesize that T cells and B cells, may synergize with each other leading to the impairment observed in coinfected mice.

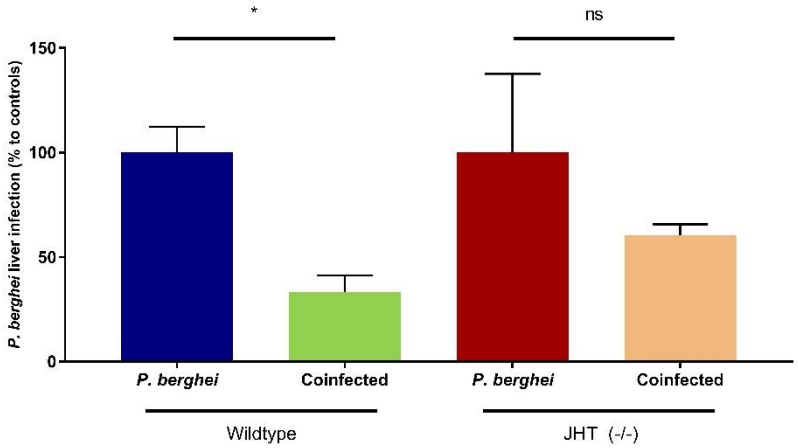

Figure 5.11 – B cells by themselves are not responsible for the impairment of *P. berghei* hepatic invasion. *P. berghei* liver load quantification 6 hours post-sporozoite injection in naïve mice (controls: WT – blue; JHT (-/-) – red) or mice infected 5 days beforehand with *T. brucei* (coinfected: WT – green; JHT (-/-) – orange). Results are expressed in means and error bars represent standard error of the mean. Mann-Whitney test between control and coinfected groups: *p<0,05; ns – not significant (n=3-4 mice per group).

- **Immune factors – IFN-γ**

To further investigate the mechanism by which *T. brucei* infection impairs hepatic invasion by *P. berghei*, we sought to identify the immune features of a *T. brucei* infection that could be involved in sporozoite elimination.

Upon a *Trypanosoma* infection, IFN-γ production by CD8+ T lymphocytes, monocytes and macrophages triggers a positive feedback loop that induces further production of IFN-γ by these subsets of cells[74,75]. Consequently, the latter cells produce trypanotoxic compounds such as NO and TNF-α, which play a major role in the control of parasitemia[48,49,50].

With this information, we hypothesized that the early induction of IFN-γ during a *T. brucei* infection may impact invasion of the host's hepatocytes by *P. berghei*. To validate our hypothesis, we compared two groups of mice which are unable to produce IFN-γ (IFN-γ (-/-)), one only infected with *P. berghei* and another infected with *T. brucei* five days prior to sporozoite injection, with two groups of wildtype mice equivalently infected. If our hypothesis was correct, we would expect to observe at least a partial recovery of the liver stage impairment phenotype in IFN-γ (-/-) coinfected mice. *Plasmodium* infection was quantified by qRT-PCR at 6 hours post-sporozoite injection. Data obtained showed a complete recovery of a normal *P. berghei* liver infection in IFN-γ (-/-) coinfected mice, contrary to what was observed in wildtype coinfected mice (105% and 38% respectively, p<0,05) (Figure 5.12).

Altogether, this data indicates that the upregulation of IFN-γ by a *Trypanosoma* infection leads to the inhibition of a subsequent *P. berghei* infection, suggesting that IFN-γ plays a pivotal role in the impairment of hepatocyte invasion by the sporozoites.

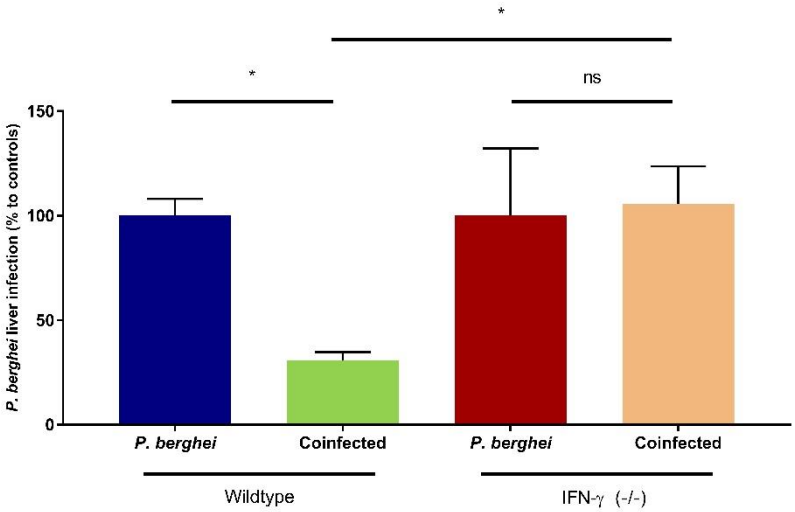

Figure 5.12 – IFN-γ is an essential immune factor, leading to the impairment of *P. berghei* hepatic invasion when present. *P. berghei* liver load quantification 6 hours post-sporozoite injection in naïve mice (controls: WT – blue; IFN-γ (-/-) – red) or mice infected 5 days beforehand with *T. brucei* (coinfected: WT – green; IFN-γ (-/-) – orange). Results are expressed in means and error bars represent standard error of the mean. Mann-Whitney test between control and coinfected groups: *p<0,05; ns – not significant (n=5 mice per group).

5.3. Assessment of the duration of the inhibitory effect of *T. brucei* lysates

The impairment of *P. berghei* liver infection observed in *T. brucei*-infected mice is also observed when *T. brucei* lysates are injected into mice 30 min prior to sporozoite inoculation (Figure 2.4). Nonetheless, the extent of protection conferred by *T. brucei* lysates remains unknown. To elucidate the duration of this inhibitory effect, *T. brucei* lysates were injected at 30 min, 6 hours, 12 hours, 24 hours and 48 hours prior to infection with *P. berghei* sporozoites, which was defined as the timepoint 0h. Furthermore, as controls we utilized a group of mice infected only with *P. berghei* and another primarily infected by *T. brucei* and, 5 days later, by *P. berghei* (coinfected). *Plasmodium* liver infection was quantified by qRT-PCR at 46 hours post sporozoite injection. We hypothesized that *T. brucei* lysates trigger a peak in the host immune response, followed by its continuous decrease, corresponding to the clearance of *T. brucei* molecules. As such, we expected that the inhibition of *P. berghei* hepatic infection by *T. brucei* lysates decreases as the time of sporozoite inoculation increases, due to a fading immune response involved in this impairment.

Our results showed a time dependent effect, where the lysates injected 30 min prior to sporozoite injection led to the highest impairment of *P. berghei* liver infection (27% of infection, p<0,001), followed by the *T. brucei* lysates injected 6 hours and 12 hours prior to *P. berghei* infection (46% and 52% of infection, respectively; p<0,01; p<0,05). Furthermore, the inhibition of *P. berghei* infection is lost when sporozoites are injected 24 to 48 hours after the administration of *T. brucei* lysates (98% and 132% respectively, not statistically significant) (Figure 5.13). Thus, we conclude that the impairment of *P. berghei* hepatic infection by *T. brucei* lysates is a time dependent phenomenon, where protection decreases as the time of between *T. brucei* lysates and sporozoite inoculation increases.

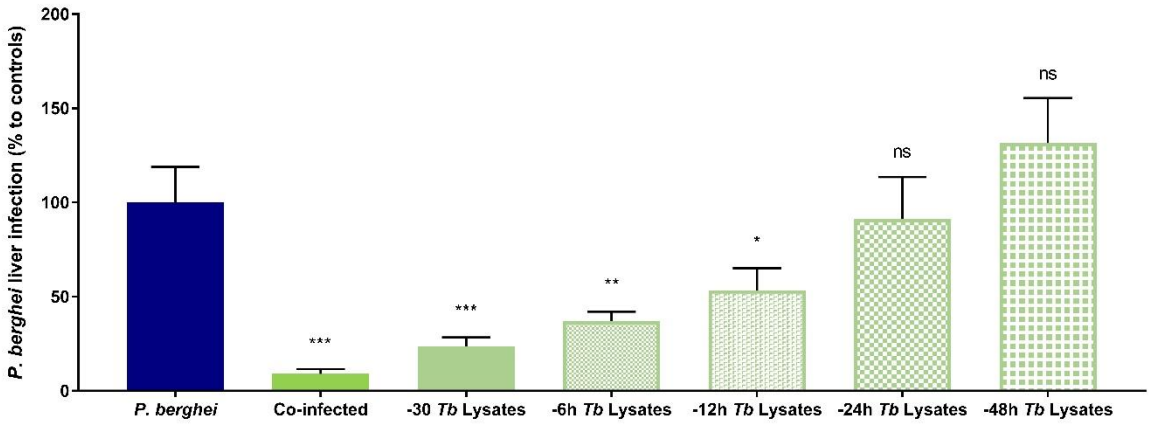

Figure 5.13 – *T. brucei* lysates protection against *P. berghei* infection is time dependent. *P. berghei* liver load quantification 46 hours post-sporozoite injection in naïve mice (controls – blue), mice infected 5 days beforehand with *T. brucei* (coinfected – green) or mice injected with *T. brucei* lysates 30 min, 6 h, 12 h, 24 h and 48 h prior to sporozoite injection (*Tb* lysates – light green patterns). Results are expressed in means and error bars represent standard error of the mean. Student's t-test between control and either coinfected or *Tb* lysates groups: ***p<0,001; **p<0.01; *p<0,05; ns – not significant (n=5 mice per group, N=2)

Next, we sought to understand if the mechanism for the overall decrease in *P. berghei* parasite liver load mediated by *T. brucei* lysates was equivalent to the mechanism at play during a *T. brucei*/*P. berghei* coinfection, which leads to a decrease in the number of EEFs in the liver, whereas *P. berghei* replication is not affected. To elucidate this, we quantified the number and size of the EEFs by immunofluorescence microscopy analysis of liver sections from mice belonging to five out of the seven groups previously studied: one single infected with *P. berghei*, as a control for infected hepatocytes per liver area and EEF size; one coinfected, as a control for *P. berghei* liver infection impairment where less EEFs are present but with equal size; one where *T. brucei* lysates were injected 30 min prior to sporozoite injection, when the impairment of *P. berghei* liver infection was higher; one with *T. brucei* lysates injection 12 hours before a subsequent *P. berghei* infection, where the impairment of *P. berghei* liver infection is present but not as strong as the previous group; and the last with *T. brucei* lysates injection 48 hours prior to sporozoite injection, where the inhibition of *P. berghei* liver infection is no longer observed.

The immunofluorescence microscopy analysis revealed a 70% reduction of the number of *Plasmodium* infected hepatocytes in the coinfected mice, at 46 hours of development, compared to those only infected by *P. berghei* (p<0,0001). Moreover, *T. brucei* lysates injected 30 min and 12 hours prior to sporozoite injection revealed 75% and 81% of reduction in the number of infected hepatocytes, respectively (p<0,0001). On the other hand, *T. brucei* lysates injected at 48h prior to sporozoite injection lead to a similar number of *Plasmodium* infected hepatocytes when compared with the controls infected with *P. berghei* only (100%; not statistically significant) (Figure 5.14). The EEFs that could be detected in all groups showed a similar parasite development to that of the group single infected with *P. berghei* (Figure 5.15 and Figure 5.16), indicating that the injection of *T. brucei* lysates has no impact on *P. berghei* replication after hepatocyte invasion. Altogether, this data was consistent with the results obtained through qRT-PCR and suggest that the mechanisms of *P. berghei* elimination are similar in the context of coinfection and injection with *T. brucei* lysates prior to *P. berghei* infection, and that this mechanism leads to elimination of *P. berghei* parasites before reaching the liver or throughout the liver stage of infection.

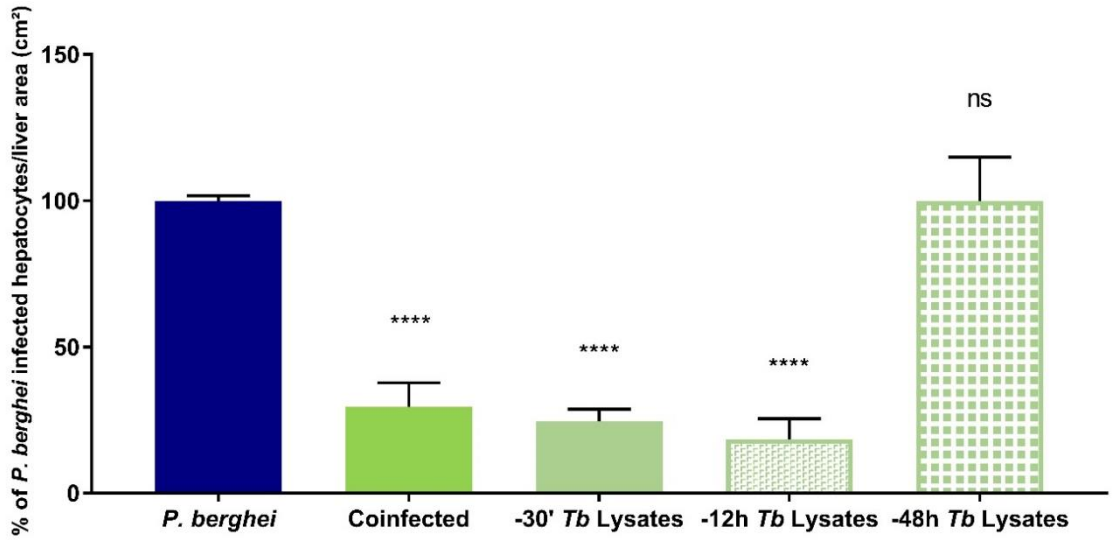

Figure 5.14 – An ongoing *T. brucei* infection and injection of *T. brucei* lysates result in a dramatic reduction of the number of *Plasmodium* EEFs. *P. berghei* EEFs microscopical quantification 46 hours post-sporozoite injection in naïve mice (controls – blue), mice infected 5 days beforehand with *T. brucei* (coinfected – green) or mice injected with *T. brucei* lysates 30 min, 12 h and 48 h prior to sporozoite injection (*Tb* lysates – light green patterns). Results are expressed in means and error bars represent standard error of the mean. Student's t-test between control and either coinfected or *Tb* lysates groups: ****p<0,0001; ns – not significant (n=5 mice per group)

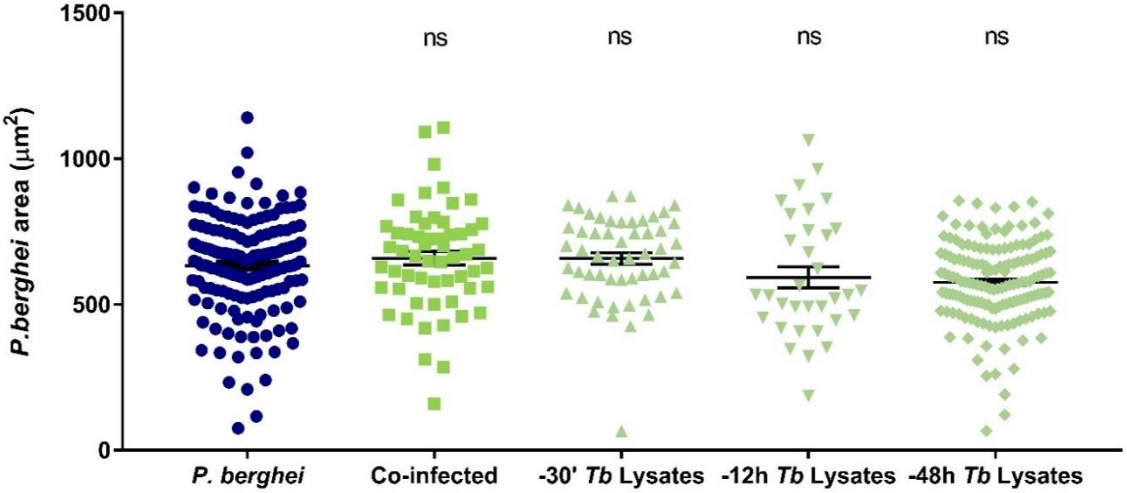

Figure 5.15 – An ongoing *T. brucei* infection and injection of *T. brucei* lysates do not result in a change of *Plasmodium* EEF size. *P. berghei* EEFs size measurement by confocal microscopy 46 hours post-sporozoite injection in naïve mice (controls – blue), mice infected 5 days beforehand with *T. brucei* (coinfected – green) or mice injected with *T. brucei* lysates 30 min, 12 h and 48 h prior to sporozoite injection (*Tb* lysates – light green patterns). Results are expressed in means and error bars represent standard error of the mean. Student's t-test between control and either coinfected or *Tb* lysates groups: ns – not significant (n=5 mice per group)

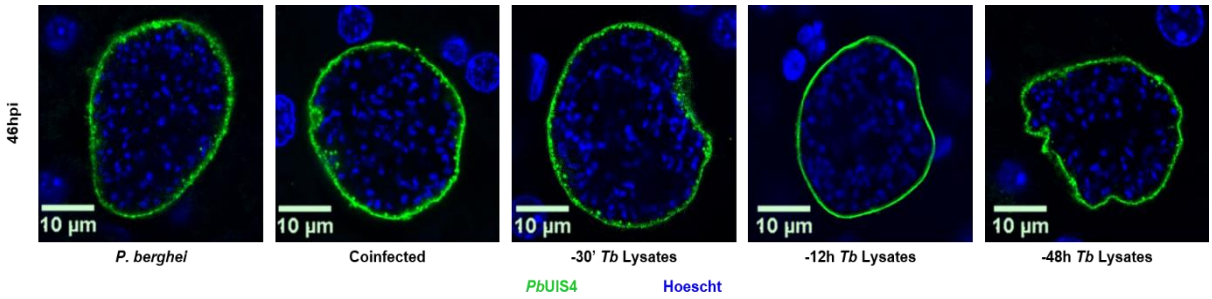

Figure 5.16 – An ongoing *T. brucei* infection and injection of *T. brucei* lysates do not result in a change of *Plasmodium* EEF size. Fluorescent microscopy imaging representative of EEFs at 46 hours post-sporozoite injection in naïve mice (controls), mice infected 5 days beforehand with *T. brucei* or mice injected with *T. brucei* lysates 30 min, 12 h and 48 h prior to sporozoite injection. Hepatocyte nuclei are depicted in blue (Hoescht staining); *P. berghei*'s parasitophorous vacuole membrane is depicted in green (Anti-UIS4). Scale bar corresponds to 10 µm.

5.4. Evaluation of cytokine profiles following coinfection and administration of *T. brucei* lysates

Since IFN-γ was shown to play a role in the impairment of *P. berghei* liver infection observed in coinfected groups we evaluated cytokine profiles of mice single infected with *P. berghei*, coinfected mice (primarily infected by *T. brucei* and, 5 days later, by *P. berghei*) and mice inoculated with *T. brucei* lysates at either 30 min, 6 hours, 12 hours, 24 hours or 48 hours prior to sporozoite injection. To do so, serum was collected at different timepoints of *P. berghei* infection: 0 hours, 6 hours, 12 hours, 24 hours and 46 hours. To account for changes in cytokine profiles resulting from *P. berghei* liver infection, serum from the group of mice infected with only *P. berghei* was collected at the same timepoints.

Even though we collected serum at the timepoints described previously, we prioritized quantification of cytokine concentrations at the following timepoints of *P. berghei* infection: 0 hours, to assess the immune environment at the moment of sporozoites injection; 12 hours, which corresponds to a timepoint where *P. berghei* replication has not yet been initiated; and 24 hours, which we hypothesize that corresponds to the peak of parasite elimination in the liver in the context of coinfection. We anticipated that at these timepoints in coinfected mice and mice injected with *T. brucei* lysates, we would observe differential cytokine levels in the profiles obtained and we hypothesized that a cytokine dose-dependent effect on *P. berghei* liver infection could be observed. Using the Q-plex assay, a panel of 16 cytokines and chemokines was quantified: IL-1α, IL-1β, IL-2, IL-3, IL-4, IL-5, IL-6, IL-10, IL-12p70, IL-17, IFN-γ, TNF-α, GM-CSF, MIP-1α, MCP-1 and RANTES. This assay is based on a traditional sandwich ELISA but performed in a multiplexed and micro scale. In Q-plex, capture antibodies are printed into a 96-well microtiter plate that bind to the target proteins in the sample (cytokines/chemokines); afterwards, detection antibodies (streptavidin horseradish peroxidase (S-HRP) pre-conjugated to the secondary antibodies) are added to these wells, which will bind to the complex formed between the capture antibody and the target cytokine. Thus, a chemiluminescent signal can be acquired, which is proportional to the amount of the targeted protein in the sample.

To determine differences in cytokine patterns induced in coinfected groups and groups injected with *T. brucei* lysates, we transformed the raw data obtained into fold change, normalizing each of the groups at the several timepoints of collection to the corresponding timepoint of *P. berghei* only infected group, so that we could exclude the influence in cytokines profiles induced by *P. berghei* liver infection. Since IL-10, IL-17, TNF-α and GM-CSF quantification ranked below the detection limit (data not shown), these cytokines were not considered for further analysis. Afterwards, to better interpret our data and observe the correlation between the different groups and cytokine expression, we performed a hierarchical clustering using complete linkage and Euclidean distance (Figure 5.17). Within this analysis, a higher proximity within the trees on the left and on the top represents a higher similarity between the groups while the heights of the branches indicate the distance between the nodes in the clustering.

Interestingly, with this clustering analysis we observed that there are two major clusters. The first cluster is represented by the cytokine profiles resulting from groups of coinfected mice (throughout all timepoints of serum collection) and the profiles resulting from the collection of serum at 0 hours from mice injected with *T. brucei* lysates no later than 12 hours. This suggests that the upregulated cytokines in these profiles may be important for the impairment of *P. berghei* liver infection mediated by *T. brucei* infection or injection of its lysates. The second cluster is represented by all the remaining groups independently of the timepoint of *T. brucei* lysates injection or serum collection, which indicate that the quantified cytokines probably do not play a major role in *P. berghei* impairment at these timepoints of infection (Figure 5.17).

Besides, we can further divide the first cluster into two subgroups based on their cytokine profile, one which includes the profiles from coinfected groups, and the other including the groups injected with *T. brucei* lysates. This division is due to the differential expression of IFN-γ, which has been shown in this work (Figure 5.12) as an important mediator in the impairment of *P. berghei* invasion of the host's hepatocytes, rendering our results more robust since it is a clear indication that *Trypanosoma* infection induces upregulation of this cytokine and goes in accord to what is known in the literature.

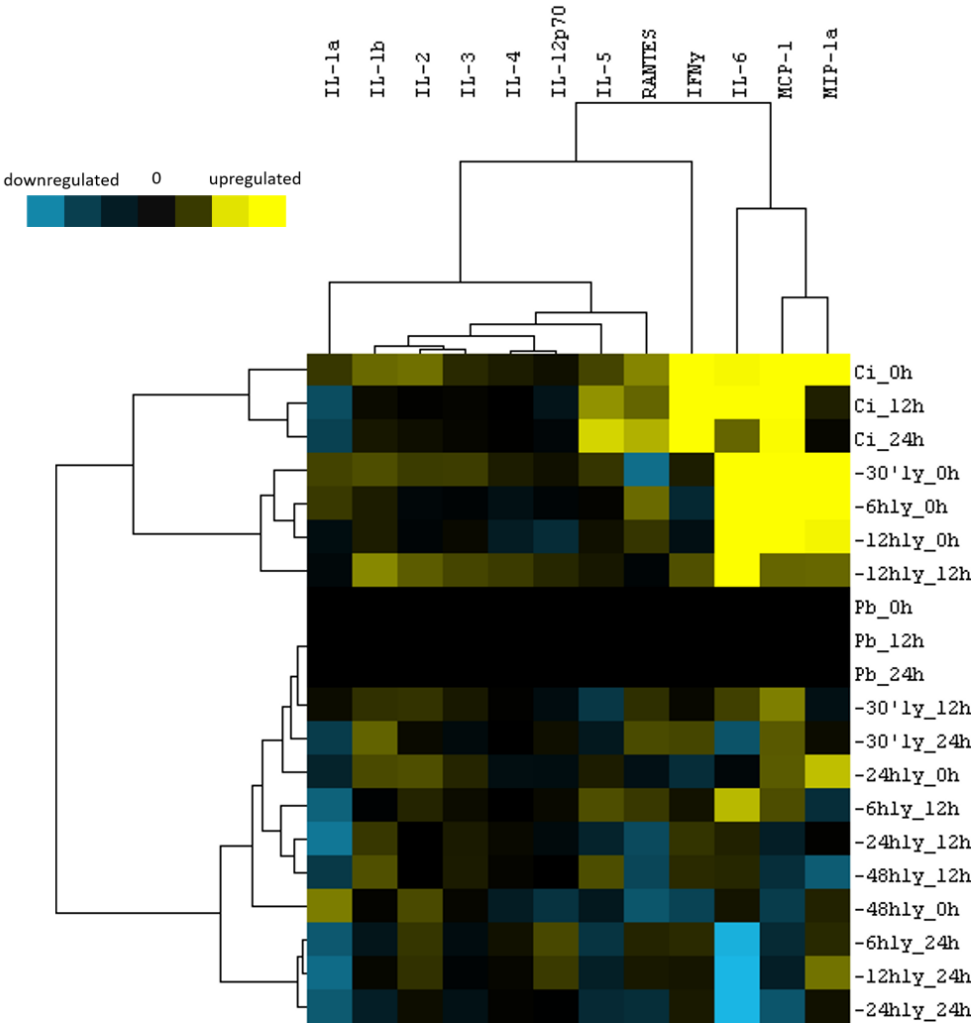

Figure 5.17 – Groups single infected with *P. berghei*, coinfected and injected with *T. brucei* lysates prior to *P. berghei* infection have different cytokines profiles. Cytokine quantification by Q-plex at 0 h, 12 h and 24 hours post-sporozoite injection in naïve mice (controls - Pb), mice infected 5 days beforehand with *T. brucei* (Coinfected – Ci) or mice injected with *T. brucei* lysates 30 min, 6 h, 12 h, 24 h and 48 h prior to sporozoite injection (-30'ly, -6hly, -12hly, -24hly and -48hly respectively). Clusters go from root at top to lead node for each cytokine and clusters in between are based on their agglomerative. Branches represent similarity, as in the shorter the branch more similar are the groups. Colours represent downregulation (blue) and upregulation (yellow).

With information of where cytokines may be playing a role in the impairment of *P. berghei* infection, we examined which cytokines seem to be relevant for this impairment. Interestingly, both MCP-1 and MIP-1α chemokines, known as chemotactic for macrophages and monocytes[112], were upregulated in coinfected and *T. brucei* lysates groups at early timepoints of serum collection (3-fold and 4-fold respectively; $p<0,05$, data not shown) when compared with groups infected with *P. berghei* only. Furthermore, the pro-inflammatory cytokine IL-6, which is typically produced by macrophages and activated T cells[66], was also upregulated, displaying a 6-fold change in concentration relative to mice single infected with *P. berghei* ($p<0,05$) (Figure 5.17). All other cytokines did not exhibit significant fold changes leading us to conclude that MCP-1, MIP-1α and IL-6 could play a role in mediating the impairment of an ongoing *P. berghei* liver infection by *T. brucei*.

5.5. Mechanism of *T. brucei*-induced impairment of an ongoing *Plasmodium* liver infection

The cytokine profiles from mice in the context of our coinfection model and in the context of the injection of lysates enabled the identification of MCP-1 and MIP-1α as candidates that may explain *P. berghei* hepatic stage impairment. As such, the section below describes our efforts to uncover the mechanism of impairment of *P. berghei* liver infection by *T. brucei.*

- **Macrophage activation**

As previously mentioned, research on *T. brucei* infection reports that macrophages play a pivotal role in the control of pathology by production of TNF-α and NO, which eliminate the parasites from circulation[48,49]. Furthermore, macrophages are also associated with elimination of *Plasmodium* EEFs[42,43,44].

MCP-1 and MIP-1α induce macrophage recruitment to locals of infection[112,113], and these chemokines were found upregulated not only in groups injected with *T. brucei* lysates prior to *P. berghei* infection, but also in the coinfected groups. As such, we hypothesize that the activation of macrophages resulting from either the injection of *T. brucei* lysates or an ongoing *T. brucei* infection, could lead to the elimination of EEFs and thereby be the responsible for the impairment observed in *P. berghei* liver infection.

To test our hypothesis, macrophages were depleted by injection of clodronate-liposomes, which are ingested by the macrophages, releasing clodronate intracellularly and leading to death by apoptosis[114]. Clodronate was administered 48 hours prior to *P. berghei* infection in two groups of mice: one single infected with *P. berghei* and another injected with *T. brucei* lysates 30 min prior to sporozoite injection. In parallel, two groups of mice were treated with PBS-liposomes and equivalently infected. *P. berghei* liver load was quantified at 46 hours post infection by qRT-PCR and clodronate treatment efficiency was assessed through the same methodology. We refrained from using a coinfected group treated with clodronate-liposomes in this experiment since these mice perish at early timepoints due to uncontrolled *T. brucei* parasitemia[51], nevertheless we added a coinfected group treated with PBS-liposomes as a control for the coinfection phenotype.

To assess the efficiency of the clodronate treatment, the following marker genes were selected: F4/80, a surface marker constitutively expressed in both peripheral and resident macrophages[115]; CD68, a surface phagocytic marker enriched in macrophages[116]; and CLEC4F, a Kupffer cell receptor, present upon entry of $F4/80^{+}$ cells in the liver[117]. Results show that F4/80 expression was lower in both clodronate-treated groups when compared with mice treated with PBS liposomes (38% for single infected with *P. berghei* and 25% for coinfected compared to the respective PBS controls; $p<0,01$ for both). CD68 quantification in clodronate-administered mice revealed a 40% reduction in mice single infected with *P. berghei* and 45% in mice injected with *T. brucei* lysates, comparing with the corresponding PBS-liposome treated groups ($p<0,05$ for both). Finally, CLEC4F quantification indicated a negligible amount of Kupffer cells in both clodronate-treated mice infected by *P. berghei* or injected with *T. brucei* lysates beforehand (15% and 2%, $p<0,01$ and $p<0,0001$ respectively) (Figure 5.18). Hence, we concluded that the depletion of liver macrophages using clodronate-liposomes was successful.

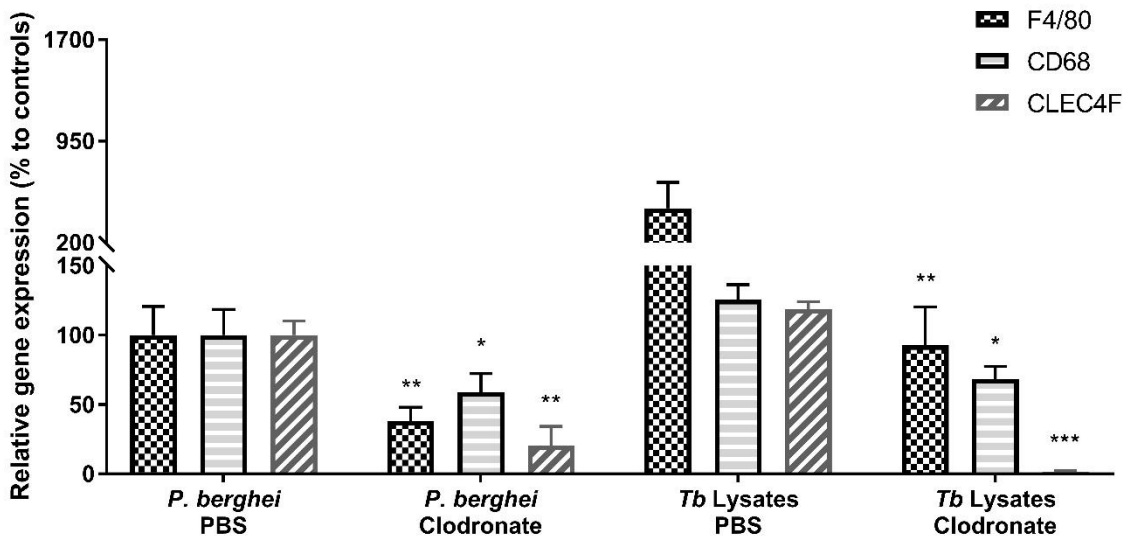

Figure 5.18 – Macrophage depletion using clodronate-liposomes was successful. Liver expression by qRT-PCR of macrophage cell marker genes: F4/80 (bars filled with squares); CD68 (bars filled with horizontal stripes); and CLEC4F (bars filled with diagonal stripes). Quantification was performed 46 hours post *P. berghei* infection in naïve mice (controls), mice infected 5 days beforehand with *T. brucei* (Coinfected) or mice injected with *T. brucei* lysates 30 min prior to sporozoite injection (*Tb* lysates), injected with PBS or treated with clodronate-liposomes 48 hours prior to sporozoite injection. Results are expressed in means and error bars represent standard error of the mean. Mann-Whitney test between control and *Tb* lysates groups: *p<0,05; **p<0,01; ***p<0,001 (n=5 mice per group)

After validating the efficiency of the macrophage depletion, we assessed the effect of macrophage depletion in the impairment of *P. berghei* liver infection by *T. brucei* lysates. If our hypothesis was proven correct, in macrophage depleted mice we would expect a full, or at least partial recovery of a normal *P. berghei* liver stage infection. The analysis revealed a similar impairment of *P. berghei* liver infection in both clodronate-treated and non-treated *T. brucei* lysates injected mice (29% and 36% respectively, not statistically significant) (Figure 5.19), leading us to conclude that macrophages do not mediate the *Trypanosoma*-dependent inhibition of *P. berghei* hepatic infection.

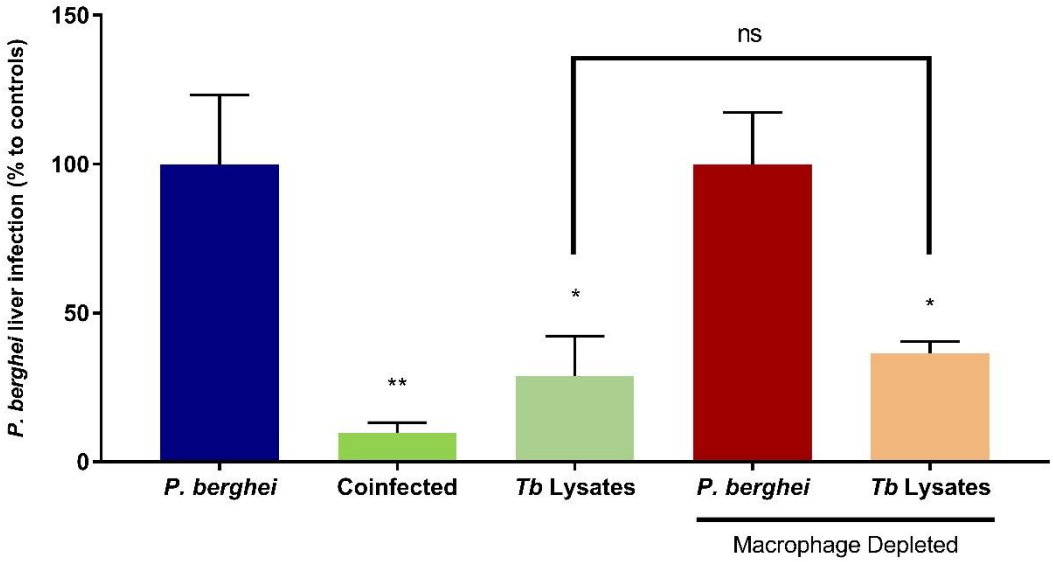

Figure 5.19 – Macrophage depletion does not rescue a normal *P. berghei* liver infection. *P. berghei* liver load quantification 46 hours post-sporozoite injection in naïve mice (controls not treated– blue; treated controls – red), mice infected 5 days beforehand with *T. brucei* (coinfected – green) or mice injected with *T. brucei* lysates 30 min prior to sporozoite injection (*Tb* lysates not treated – light green; *Tb* lysates treated – orange). Results are expressed in means and error bars represent standard error of the mean. Mann-Whitney between control and either coinfected or *Tb* lysates groups: **p<0.01; *p<0,05; (n=5 mice per group)

- **Monocyte activation**

Even though our data showed that macrophages did not play a role in the impairment of *Plasmodium* liver infection by *T. brucei*, we hypothesized that monocytes produced post-clodronate treatment could be mediating this impairment, since monocytes have been shown to be involved in the defence against *Plasmodium* liver infection[38] and both MCP-1 and MIP-1α are chemoattractant for this subset of cells[112]. To test our hypothesis, we administered α-CCR2 antibody which does not allow monocyte recruitment through blocking of the CCR2 receptor[48,118]. This antibody was injected at 48 and 24 hours prior to *P. berghei* infection, upon *P. berghei* infection, and 24 hours post *P. berghei* infection[118] in three groups of mice: one infected only with *P. berghei*; one coinfected (primarily infected by *T. brucei* and, 5 days later, by *P. berghei*); and one injected with *T. brucei* lysates 30 min prior to sporozoite injection. In parallel, PBS 1x, the antibody vehicle, was administered to three equivalent groups of mice. *P. berghei* liver load was quantified at 46 hours post infection by qRT-PCR and depletion efficiency was assessed by flow cytometry.

Monocytes can be distinguished by their functions, according to the presence of specific markers such as CD11b, LY6C and CCR2[119]. Monocytes are recognized by their high expression of CD11b and LY6C markers and are termed $CD11b^{+}LY6C^{+}$ [48]. As such, for the flow cytometry analysis the gating strategy chosen was based primarily on a viability dye, which allowed us to exclude dead cells from the quantification, followed by exclusion of all but single cells, and finishing with a gate for $CD11b^{+}$ and $LYC6^{+}$ markers which allowed us to identify the inflammatory monocyte population (Supplementary Figure 1) Flow cytometry analysis of mice treated with the α-CCR2 antibody showed that the liver monocytes ($CD11b^{+}LY6C^{+}$ cell population) were reduced by 68% in the group infected with *P. berghei* only ($p<0,05$), 72% in the coinfected group ($p<0,01$) and 61% in the group injected with *T. brucei* lysates ($p<0,05$) when compared to their respective controls injected with PBS 1x (Figure 5.20 and Supplementary Figure 2). Therefore, we concluded that the blockage of recruitment of liver monocytes was successful.

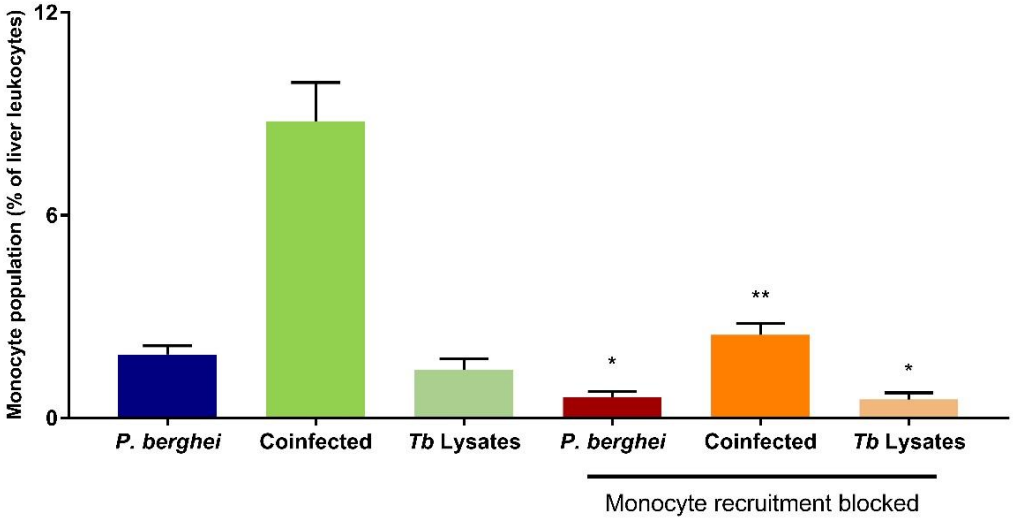

Figure 5.20 – Blockage of monocyte recruitment using α-CCR2 antibody was successful. Monocyte population quantification by flow cytometry. Quantification was performed 46 hours post *P. berghei* infection in naïve mice (controls not depleted – blue; depleted – red), mice infected 5 days beforehand with *T. brucei* (Coinfected not depleted – green; depleted – orange) or mice injected with *T. brucei* lysates 30 min prior to sporozoite injection (*Tb* lysates not depleted – light green; depleted – light orange). Results are expressed in means and error bars represent standard error of the mean. Mann-Whitney test between control and *Tb* lysates groups: *$p<0,05$; **$p<0,01$ (n=5 mice per group)

We then assessed the effect of blocking monocyte recruitment on the impairment of *P. berghei* liver infection by *T. brucei* lysates or in the context of a *P. berghei*/*T. brucei* coinfection. If monocytes were, in fact, mediating the impairment of *P. berghei* liver infection by *T. brucei*, then we should see at least a partial recovery of *P. berghei* liver stage infection in mice whose monocyte recruitment had been

blocked. Surprisingly, data revealed that *P. berghei* liver infection inhibition was still present in mice previously infected with *T. brucei* or injected with *T. brucei* lysates (15% and 11% of infection, relative to a treated control single infected with *P. berghei*, respectively; $p<0,05$ and $p<0,01$) (Figure 5.21).

Since we were unable to rescue *P. berghei* liver infection through the blockage of monocyte recruitment, we concluded that neither macrophages nor monocytes are responsible for the *Trypanosoma*-mediated impairment of *P. berghei* infection and that MCP-1 and MIP-1α do not play a major role in the coinfection phenotype.

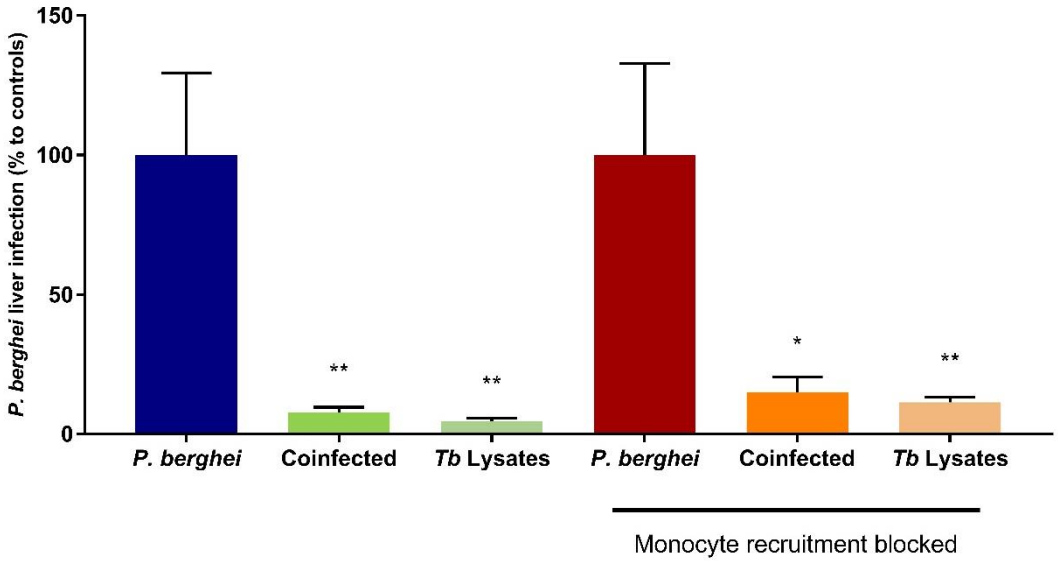

Figure 5.21 – Blockage of monocyte recruitment does not rescue a normal *P. berghei* liver infection. *P. berghei* liver load quantification 46 hours post-sporozoite injection in naïve mice (controls not treated – blue; treated controls – red), mice infected 5 days beforehand with *T. brucei* (coinfected not treated – green) or mice injected with *T. brucei* lysates 30 min prior to sporozoite injection (*Tb* lysates not treated – light green; *Tb* lysates treated – orange). Results are expressed in means and error bars represent standard error of the mean. Mann-Whitney test between control and either coinfected or *Tb* lysates groups: **p<0.01; *p<0,05; (n=5 mice per group)

6. CONCLUSIONS AND FUTURE PERSPECTIVES

Although malaria and sleeping sickness are coendemic in various African regions[78,91,92], the coinfections between *Plasmodium* and *Trypanosoma brucei* remain poorly investigated. To date, a single study attempted to understand the interactions between these pathogens *in vivo* and revealed an aggravation of symptoms, such as stronger anemia, and decrease of survival times of mice infected simultaneously with *T. brucei* and *P. berghei* blood stage parasites[78]. Interestingly, research by the host lab revealed that both an ongoing *T. brucei* infection and the injection of *T. brucei* lysates lead to the impairment of a subsequent *P. berghei* liver infection. Furthermore, previous data showed that this impairment is likely mediated by the host's immune system, which may play a role in two different stages of the infective process: impairing hepatocyte invasion by *P. berghei* and eliminating *P. berghei* during an ongoing infection. Therefore, the goal of the present work was to characterize the impact of the host's immune response to *T. brucei* that results in the impairment of *P. berghei* liver infection.

In vitro models provide opportunities to study specific cellular responses in closed and controlled systems. As such, we adapted a previously employed model and attempted the establishment of a novel *in vitro* system by combining splenocytes and serum from *T. brucei*-infected mice. This attempt to add immune components while emulating the coinfection setup *in vitro* did not reveal an impairment of *P. berghei* hepatic infection that could be attributed to splenocytes and/or serum from mice infected with *T. brucei*. This is possibly due to the complex interplay between host cells, such as hepatocytes, endothelial and Kupffer cells which may be pivotal for the phenotype observed *in vivo*. Therefore, we attempted to implement a novel *in vitro* system based on mouse liver slice cultures, which retain the original liver tissue structure with all its resident cell types[111]. However, loss of liver slice viability constituted as a major hurdle, which might be explained by the setup used in this work, which differs from that described in the literature. The major differences reported are: utilization of a sectioning device whose sections are not exact in shape nor size; and usage of a preserving solution that is not ideal for liver preservation. The loss of liver slice viability might be overcome in the future by utilizing a sectioning device with strict section measurements, as well as an optimal liver preserving solution, such as University of Wisconsin organ preserving solution[105] to perfuse the mice before collection of the livers.

Without an *in vitro* system that emulates the coinfection setup, our focus was centred on the comprehension of the involvement of the immune system in the interplay between a *T. brucei*/*P. berghei* coinfection by employing murine models. To uncover the influence of the *T. brucei* on the impairment of *P. berghei* hepatocyte invasion, we further investigated previous indications that coinfected murine models lacking T and B cells recovered a normal *P. berghei* hepatic infection at 6 hours post-sporozoite injection. T cells are acknowledged as key players in the control of both a *T. brucei* infection[50] and a *P. berghei* hepatic infection[16]. By establishing a coinfection between *T. brucei* and *P. berghei* in wildtype mice and different murine models, each lacking different T cell subsets, we did not observe a recovery of a normal *P. berghei* liver infection in these mice, leading us to conclude that each T cell subset alone had no significant impact on the *T. brucei*-mediated impairment of hepatocyte invasion by *P. berghei*. B cells still remained as a possible candidate for the inhibition of hepatocyte invasion by *P. berghei* mediated by *T. brucei*. Therefore, we employed mice lacking B cells to attempt to rescue *P. berghei* liver infection in coinfected mice. In these murine models, we did not observe a normal *P. berghei* infection and, hence, we concluded that neither T nor B cells play a role mediating this impairment by themselves. As such, we hypothesize that compensatory mechanisms between αβ T cells and γδ T cells might be at play, since their synergy has been described in a study where immunized mice lacking both subsets of immune cells did not present protective immunity against sporozoite challenge, whilst wildtype mice showed protection against infection[120]. To test this hypothesis, simultaneous depletion of

αβ T cells and γδ T cells could be attempted. If our hypothesis is correct, a coinfection setup in these mice would reveal a normal *P. berghei* liver infection.

Furthermore, quantification of expression of inflammatory molecules present in the liver performed by the host lab suggested that changes induced by a *T. brucei* infection could be responsible for the inhibition of *P. berghei* hepatic infection. As such, to further investigate *P. berghei* hepatic invasion impairment caused by an ongoing *T. brucei* infection, we prioritized the search for immune features of *T. brucei* infection that could be involved in sporozoite elimination. Previous studies showed that during a *T. brucei* infection, $CD8^+$ lymphocytes and macrophages produce IFN-γ in a positive feedback loop[48,49]. Furthermore, IFN-γ is also responsible for the elimination of liver stage *Plasmodium* parasites through NO production[68]. Based on this information, we employed mice unable to produce IFN-γ in our coinfection setup and we observed that coinfected IFN-γ (-/-) mice completely recovered a normal *P. berghei* liver infection at 6 hours post-sporozoite injection. Therefore, this result showed that IFN-γ produced by the host in response to a *T. brucei* infection is involved in the inhibition of hepatocyte invasion by the sporozoites. To elucidate the mechanism by which IFN-γ interferes with hepatocyte invasion by *P. berghei*, mice that produce IFN-γ but lack its receptor could be utilized. In case IFN-γ acts directly on the sporozoites, then an impairment in *P. berghei* liver infection would still be observed in these mice. On the other hand, if IFN-γ is only a mediator, then the coinfected mice should reveal a normal *P. berghei* infection, since IFN-γ would not be able to link to its receptor and induce a subsequent response which then affects the sporozoites.

To further understand the involvement of the immune system in the interplay between *T. brucei* and *P. berghei* infections, we assessed the protection conferred by the injection of *T. brucei* lysates prior to *P. berghei* infection. We hypothesized that this protection is due to a peak of an immune response, followed by a continuous decrease, corresponding to the clearance of *T. brucei* molecules. To test this hypothesis, mice were injected with *T. brucei* lysates at several timepoints prior to sporozoite injection, and *P. berghei* liver load was quantified at 46 hours post infection. Our data revealed that the impairment of *P. berghei* liver infection observed is a time dependent event, where lysates injected 24 to 48 hours prior to sporozoite injection no longer induce a protective effect. Moreover, we unveiled that the protection conferred by *T. brucei* lysates is due to a decrease in the number of infected hepatocytes and that this protective effect decreases as the time of injection prior to *P. berghei* infection increases. Furthermore, immunofluorescence analysis of liver sections also showed that *T. brucei* lysates do not impact *P. berghei* replication inside the hepatocytes. These results are in accordance to those obtained previously, where livers from mice infected with *T. brucei* 5 days prior to a *P. berghei* infection were compared with livers from mice singly infected with *P. berghei*. Altogether, these results suggest similar mechanisms of *P. berghei* elimination in both *T. brucei*/*P. berghei* coinfection and *T. brucei* lysates injection setup. To further understand whether sporozoites are eliminated while homing the liver or after they have infected hepatocytes, quantification of *P. berghei* hepatic infection could be performed in livers collected 30min after sporozoite injection. We expect that if a similar number of hepatocytes is found at this timepoint in mice infected with *P. berghei* only and in mice injected with *T. brucei* lysates prior to *P. berghei* infection, then parasite elimination likely occurs during an ongoing infection.

Since IFN-γ had been shown to be involved in the impairment of hepatocyte invasion by *P. berghei* in coinfected mice, we sought to understand the impact of cytokines in the impairment of an ongoing *P. berghei* infection by *T. brucei*. Our goals were to unravel if cytokine profiles were related with the differential inhibitory effect on *P. berghei* liver infection of *T. brucei* lysates injected at several timepoints. To this end, we collected serum from mice either infected with *T. brucei* or injected with *T. brucei* lysates at several timepoints prior to *P. berghei* infection and quantified cytokine concentrations at various timepoints during an ongoing *P. berghei* infection. MCP-1, MIP-1α and IL-6 were found to be upregulated in the groups where an impairment in *P. berghei* infection had been observed through quantification by qRT-PCR, indicating their possible involvement in *P. berghei* hepatic infection

impairment by *T. brucei*. Taking into consideration the fact that both MCP-1 and MIP-1α are chemokines that induce the recruitment of macrophages and monocytes to the site of infection[112], and that macrophages play a major role in the elimination of *P. berghei*[42,43], we hypothesized that these cells might be involved in the impairment of *P. berghei* liver infection by *T. brucei*. However, contrarily to what we expected, macrophage depletion did not lead to a normal *P. berghei* liver infection in coinfected mice, indicating that either these cells were not responsible for the elimination or that recruited monocytes could be playing a role in this process. We then assessed whether monocytes could be mediating the impairment observed in coinfected mice by infecting mice whose monocyte recruitment had been blocked by specific antibodies. Surprisingly, we were unable to rescue *P. berghei* liver infection in coinfected mice whose monocyte recruitment had been blocked. We hypothesize that this could be due to the presence of macrophages in these mice, therefore a simultaneous depletion of macrophages and monocytes could be employed in order to assess if the absence of both these types of cells leads to the recovery of a normal *P. berghei* infection in coinfected mice. Moreover, IL-6, which was found upregulated in mice that revealed an inhibition in *P. berghei* liver infection, remains as a possible candidate mediating this impairment and, as such, future studies should assess the involvement of this cytokine in the interaction between an ongoing *T. brucei* infection and a subsequent *P. berghei* infection.

In summary, the present work was able to demonstrate that the host's immune system is mediating the impairment of *P. berghei* infection by responding to an ongoing *T. brucei* infection and the injection of *T. brucei* lysates. Namely, our results reveal that upon suppression of IFN-γ production, an immune response to *T. brucei*, a normal invasion of the hepatocytes by *P. berghei* is rescued in mice coinfected with *T. brucei* and *P. berghei*. Furthermore, our data strongly suggests the involvement of cytokines mediating the elimination of sporozoites/EEFs during an ongoing *P. berghei* infection due to differential cytokine expression in mice where *P. berghei* hepatic infection was impaired. Nevertheless, the underlying mechanism regarding the elimination of *P. berghei* parasites after hepatocyte invasion remains unclear and should be examined in depth.

7. REFERENCES

1. World Health Organization. *World Malaria Report 2017*. (2017).
2. Cowman, A. F., Healer, J., Marapana, D. & Marsh, K. Malaria: Biology and Disease. *Cell* **167,** 610–624 (2016).
3. Prudêncio, M., Mota, M. M. & Mendes, A. M. A toolbox to study liver stage malaria. *Trends Parasitol* **27,** 565–574 (2011).
4. Nadjm, B. & Behrens, R. H. Malaria: An Update for Physicians. *Infect. Dis. Clin. North Am.* **26,** 243–259 (2012).
5. Rénia, L. & Goh, Y. S. Malaria parasite: the great escape. *Front. Immunol.* **7,** 463 (2016).
6. Arévalo-Herrera, M., Chitnis, C. & Herrera, S. Current status of *Plasmodium vivax* vaccine. *Hum. Vaccin.* **6,** 124–132 (2010).
7. Schofield, L. & Grau, G. E. Immunological processes in malaria pathogenesis. *Nat. Rev. Immunol.* **5,** 722–735 (2005).
8. Singh, B. *et al.* A large focus of naturally acquired *Plasmodium knowlesi* infections in human beings. *Lancet* **363,** 1017–1024 (2016).
9. Brasil, P. *et al.* Outbreak of human malaria caused by *Plasmodium simium* in the Atlantic Forest in Rio de Janeiro: A molecular epidemiological investigation. *Lancet Glob. Heal.* (2017). doi:10.1016/S2214-109X(17)30333-9
10. Prudêncio, M., Rodriguez, A. & Mota, M. M. The silent path to thousands of merozoites: the *Plasmodium* liver stage. *Nat. Rev. Microbiol.* **4,** 849–856 (2006).
11. Ménard, R. *et al.* Looking under the skin: The first steps in malarial infection and immunity. *Nat. Rev. Microbiol.* **11,** 701–712 (2013).
12. Hafalla, J. C., Silvie, O. & Matuschewski, K. Cell biology and immunology of malaria. *Immunol. Rev.* **240,** 297–316 (2011).
13. Vaughan, A. M. & Kappe, S. H. I. Malaria Parasite Liver Infection and Exoerythrocytic Biology. *Cold Spring Harb Perspect Med.* **7,** a025486 (2017).
14. Zuzarte-Luis, V., Mota, M. M. & Vigário, A. M. Malaria infections: What and how can mice teach us. *J. Immunol. Methods* **410,** 113–122 (2014).
15. *Plasmodium* life cycle. Available at: http://www.cddep.org/tool/life_cycle_malaria_parasite. (Accessed: 13th July 2018)
16. Holz, L. E., Fernandez-Ruiz, D. & Heath, W. R. Protective immunity to liver-stage malaria. *Clin. Transl. Immunol.* **5,** e105 (2016).
17. Coppi, A. *et al.* Heparan Sulfate Proteoglycans Provide a Signal to *Plasmodium* Sporozoites to Stop Migrating and Productively Invade Host Cells. *Cell Host Microbe* **2,** 316–327 (2007).
18. Lindner, S. E., Miller, J. L. & Kappe, S. H. I. Malaria parasite pre-erythrocytic infection: Preparation meets opportunity. *Cell. Microbiol.* **14,** 316–324 (2012).
19. Tavares, J. *et al.* Role of host cell traversal by the malaria sporozoite during liver infection. *J. Exp. Med.* **210,** 905–915 (2013).
20. Risco-Castillo, V. *et al.* Malaria sporozoites traverse host cells within transient vacuoles. *Cell Host Microbe* **18,** 593–603 (2015).
21. Kaushansky, A. & Kappe, S. H. I. Selection and refinement: 0The malaria parasite's infection and exploitation of host hepatocytes. *Curr. Opin. Microbiol.* **26,** 71–78 (2015).
22. Nyboer, B., Heiss, K., Mueller, A. K. & Ingmundson, A. The *Plasmodium* liver-stage parasitophorous vacuole: A front-line of communication between parasite and host. *Int. J. Med. Microbiol.* **308,** 107–117 (2017).
23. Kaushansky, A. *et al.* Malaria parasite liver stages render host hepatocytes susceptible to mitochondria-initiated apoptosis. *Cell Death Dis.* **4,** e762-9 (2013).
24. Sturm, A. *et al.* Manipulation of host hepatocytes by the malaria parasite for delivery into liver sinusoids. *Science (80-.).* **313,** 1287–1290 (2006).
25. Ponte-Sucre, A. An overview of *Trypanosoma brucei* infections: An intense host-parasite interaction. *Front. Microbiol.* **7,** 1–12 (2016).
26. Morrison, L. J., Vezza, L., Rowan, T. & Hope, J. C. Animal African Trypanosomiasis: Time to Increase Focus on Clinically Relevant Parasite and Host Species. *Trends Parasitol.* **32,** 599–607 (2016).

27. Franco, J. R. *et al.* Monitoring the elimination of human African trypanosomiasis: Update to 2014. *PLoS Negl. Trop. Dis.* **11,** e0005585 (2017).
28. Oluwafemi et al., 2007. The impact of African animal trypanosomosis and tsetse on the livelihood and well-being of cattle and their owners in the BICOT study area of Nigeria. *Sci. Res. Essay* **2,** 380–383 (2007).
29. Lundkvist, G. B., Kristensson, K. & Bentivoglio, M. Why trypanosomes cause sleeping sickness. *Physiology (Bethesda).* **19,** 198–206 (2004).
30. Sleeping sickness geographical distribution. Available at: http://gamapserver.who.int/mapLibrary/app/searchResults.aspx. (Accessed: 13th July 2018)
31. MacGregor, P., Savill, N. J., Hall, D. & Matthews, K. R. Transmission stages dominate trypanosome within-host dynamics during chronic infections. *Cell Host Microbe* **9,** 310–318 (2011).
32. Trindade, S. *et al. Trypanosoma brucei* Parasites Occupy and Functionally Adapt to the Adipose Tissue in Mice. *Cell Host Microbe* **19,** 837–848 (2016).
33. Wohlleber, D. & A. Knolle, P. *Infection, Immune Homeostasis and Immune Privilege*. *Springer* (Birkhauser Advances in Infectious Diseases, 2012). doi:10.1007/978-3-0348-0445-5_2
34. Nemeth, E., Baird, A. W. & O'Farrelly, C. Microanatomy of the liver immune system. *Semin. Immunopathol.* **31,** 333–343 (2009).
35. Bertolino, P. & Bowen, D. G. Malaria and the liver: Immunological hide-and-seek or subversion of immunity from within? *Front. Microbiol.* **6,** 1–15 (2015).
36. Stijlemans, B., Radwanska, M., Trez, C. De & Magez, S. African trypanosomes undermine humoral responses and vaccine development: Link with inflammatory responses? *Front. Immunol.* **8,** 1–14 (2017).
37. Geiger, A. *et al.* Escaping deleterious immune response in their hosts: Lessons from *Trypanosoma*tids. *Front. Immunol.* **7,** 1–21 (2016).
38. Tannous, S. & Ghanem, E. A bite to fight: front-line innate immune defenses against malaria parasites. *Pathog. Glob. Health* **112,** 1–12 (2018).
39. Rocha, B. C. *et al.* Type I Interferon Transcriptional Signature in Neutrophils and Low-Density Granulocytes Are Associated with Tissue Damage in Malaria. *Cell Rep.* **13,** 2829–2841 (2015).
40. Stevenson, M. M. & Riley, E. M. Innate immunity to malaria. *Nat. Rev. Immunol.* **4,** 169–180 (2004).
41. Taylor, P. R. *et al.* Macrophage receptors and immune recognition. *Annu. Rev. Immunol.* (2005). doi:10.1146/annurev.immunol.23.021704.115816
42. Frevert, U. & Nardin, E. Cellular effector mechanisms against *Plasmodium* liver stages. *Cell. Microbiol.* **10,** 1956–1967 (2008).
43. De Souza, J. B. Protective immunity against malaria after vaccination. *Parasite Immunol.* **36,** 131–139 (2014).
44. Corradin, G. & Levitskaya, J. Priming of CD8+T cell responses to liver stage malaria parasite antigens. *Front. Immunol.* **5,** 1–6 (2014).
45. Helming, L. Inflammation: Cell Recruitment versus local proliferation. *Curr. Biol.* **21,** R548–R550 (2011).
46. Harris, T. H., Mansfield, J. M. & Paulnock, D. M. CpG oligodeoxynucleotide treatment enhances innate resistance and acquired immunity to African trypanosomes. *Infect. Immun.* **75,** 2366–2373 (2007).
47. Drennan, M. B. *et al.* The Induction of a Type 1 Immune Response following a *Trypanosoma brucei* Infection Is MyD88 Dependent. *J. Immunol.* **175,** 2501–2509 (2005).
48. Bosschaerts, T. *et al.* Tip-DC development during parasitic infection is regulated by IL-10 and requires CCL2/CCR2, IFN-γ and MyD88 signaling. *PLoS Pathog.* **6,** 35–36 (2010).
49. Quan, N. *et al.* Chronic overexpression of proinflammatory cytokines and histopathology in the brains of rats infected with *Trypanosoma brucei*. *J. Comp. Neurol.* **414,** 114–130 (1999).
50. Namangala, B., Noël, W., De Baetselier, P., Brys, L. & Beschin, A. Relative Contribution of Interferon-γ and Interleukin-10 to Resistance to Murine African Trypanosomosis. *J. Infect. Dis.* **183,** 1794–1800 (2001).
51. Sanches-Vaz, M. *et al.* Data not published.
52. Stijlemans, B. *et al.* MIF Contributes to *Trypanosoma brucei* Associated Immunopathogenicity

Development. *PLoS Pathog.* **10,** (2014).
53. Caljon, G. *et al.* Neutrophils enhance early *Trypanosoma brucei* infection onset. *Sci. Rep.* **8,** 11203 (2018).
54. Actor, J. K. *Introductory Immunology Basic Concepts for Interdisciplinary Applications*. (Academic Press, 2014). doi:10.1016/B978-0-12-420030-2.00010-X
55. Dups, J. N., Pepper, M. & Cockburn, I. A. Antibody and B cell responses to *Plasmodium* sporozoites. *Front. Microbiol.* **5,** 1–7 (2014).
56. Dong, C., Martinez, G. J. & T, C. T cells : the usual subsets. *Nat. Rev. Immunol.* **54,** 1 (2010).
57. Tsuji, M. & Zavala, F. γδ-T cells as mediators of protective immunity against liver stages of *Plasmodium*. *Trends Parasitol.* **19,** 88–93 (2003).
58. Valmori, D. V. *et al.* Induction of a cytotoxic T cell response by co-injection of a T helper peptide and a cytotoxic T lymphocyte peptide in incomplete Freund's adjuvant (IFA): further enhancement by pre-injection of IFA alone. *Eur. J. Immunol.* 1458–1462 (1994). doi:10.1016/B978-155860700-2.50002-1
59. McKenna, K. C. *et al.* Gd-T cells are a component of early immunity against preerythrocytic malaria parasites. *Infect. Immun.* **68,** 2224–2230 (2000).
60. Guilliams, M. *et al.* Experimental Expansion of the Regulatory T Cell Population Increases Resistance to African Trypanosomiasis. *J. Infect. Dis.* **198,** 781–791 (2008).
61. Shoda, L. K. M. *et al.* DNA from protozoan parasites *Babesia bovis*, *Trypanosoma cruzi*, and *T. brucei* is mitogenic for B lymphocytes and stimulates macrophage expression of interleukin-12, tumor necrosis factor alpha, and nitric oxide. *Infect. Immun.* **69,** 2162–2171 (2001).
62. Reinitz, D. M. & Mansfield, J. M. T-cell-independent and T-cell-dependent B-cell responses to exposed variant surface glycoprotein epitopes in trypanosome-infected mice. *Infect. Immun.* **58,** 2337–2342 (1990).
63. Magez, S. *et al.* The role of B-cells and IgM antibodies in parasitemia, anemia, and VSG switching in *Trypanosoma brucei*-infected mice. *PLoS Pathog.* **4,** (2008).
64. Horn, D. Antigenic variation in African trypanosomes. *Mol. Biochem. Parasitol.* **195,** 123–129 (2014).
65. Mugnier, M. R., Cross, G. A. M. & Papavasiliou, F. N. The in vivo dynamics of antigenic variation in *Trypanosoma brucei*. *Science (80-.).* **347,** 1470–1473 (2015).
66. Zhang, J.-M. & An, J. Cytokines, Inflammation and Pain. *Int Anesth. Clin.* **45,** 27–37 (2007).
67. Doolan, D. L. & Hoffman, S. L. The Complexity of Protective Immunity Against Liver-Stage Malaria. *J. Immunol.* **165,** 1453–1462 (2000).
68. Miller, J. L., Sack, B. K., Baldwin, M., Vaughan, A. M. & Kappe, S. H. I. Interferon-Mediated Innate Immune Responses against Malaria Parasite Liver Stages. *Cell Rep.* **7,** 436–447 (2014).
69. Hanum, S. P., Hayano, M. & Kojima, S. Cytokine and chemokine responses in a cerebral malaria-susceptible or -resistant strain of mice to *Plasmodium berghei* ANKA infection: Early chemokine expression in the brain. *Int. Immunol.* **15,** 633–640 (2003).
70. Frevert, U. & Krzych, U. *Plasmodium* cellular effector mechanisms and the hepatic microenvironment. *Front. Microbiol.* **6,** 1–19 (2015).
71. Nussler, A. *et al.* TNF inhibits malaria hepatic stages *in vitro* via synthesis of IL-6. *Int. Immunol.* **3,** 317–321 (1991).
72. Pied, S., Renia, L., Nussler, A., Miltgen, F. & Mazier, D. Inhibitory activity of IL-6 on malaria hepatic stages. *Parasite Immunol.* **13,** 211–217 (1991).
73. Depinay, N. *et al.* Inhibitory effect of TNF-α on malaria pre-erythrocytic stage development: Influence of host hepatocyte/parasite combinations. *PLoS One* **6,** (2011).
74. Olsson, T. *et al.* CD8 is critically involved in lymphocyte activation by a T. brucei brucei-released molecule. *Cell* **72,** 715–727 (1993).
75. Bakhiet, M. *et al.* Human and rodent interferon-gamma as a growth factor for *Trypanosoma brucei*. *Eur. J. Immunol.* **26,** 1359–64 (1996).
76. Vanwalleghem, G., Morias, Y., Beschin, A., Szymkowski, D. E. & Pays, E. *Trypanosoma brucei* growth control by TNF in mammalian host is independent of the soluble form of the cytokine. *Sci. Rep.* **7,** 1–7 (2017).
77. Griffiths, E. C., Pedersen, A. B., Fenton, A. & Petchey, O. L. The nature and consequences of coinfection in humans. *J. Infect.* **63,** 200–206 (2011).

78. Ademola, I. O. & Odeniran, P. O. Co-infection with *Plasmodium berghei* and *Trypanosoma brucei* increases severity of malaria and trypanosomiasis in mice. *Acta Trop.* **159,** 29–35 (2016).
79. Rollinson, D. *Advances in parasitology*. (Oxford: Academic Press, 2014).
80. Mwangi, T. W., Bethony, J. M. & Brooker, S. Malaria and helminth interactions in humans: an epidemiological viewpoint. *Ann. Trop. Med. Parasitol.* **100,** 551–570 (2006).
81. Poulin, R. *Parasite Manipulation of Host Behavior: An Update and Frequently Asked Questions*. *Advances in the Study of Behavior* **41,** (Elsevier Inc., 2010).
82. Faber, M. T. *et al.* Genital chlamydia, genital herpes, trichomonas vaginalis and gonorrhea prevalence, and risk factors among nearly 70,000 randomly selected women in 4 nordic countries. *Sex. Transm. Dis.* **38,** 727–734 (2011).
83. Gong, L. *et al.* Evidence for both innate and acquired mechanisms of protection from *Plasmodium falciparum* in children with sickle cell trait. *Blood* **119,** 3808–3814 (2013).
84. Degarege, A. *et al. Plasmodium falciparum* and soil-transmitted helminth co-infections among children in sub-Saharan Africa: a systematic review and meta-analysis. *Parasit. Vectors* **9,** 344 (2016).
85. Burdam, F. H. *et al.* Asymptomatic *vivax* and falciparum parasitaemia with helminth co-infection: Major risk factors for anaemia in early life. *PLoS One* **11,** 1–15 (2016).
86. Cox, F. E. Concomitant infections, parasites and immune responses. *Parasitology* **122 Suppl,** S23--S38 (2001).
87. Page, K. R., Scott, A. L. & Manabe, Y. C. The expanding realm of heterologous immunity: Friend or foe? *Cell. Microbiol.* **8,** 185–196 (2006).
88. Frischknecht, F. & Fackler, O. T. Experimental systems for studying *Plasmodium*/HIV coinfection. *FEBS Lett.* **590,** 2000–2013 (2016).
89. Portugal, S. *et al.* Host-mediated regulation of superinfection in malaria. *Nat. Med.* **17,** 732–737 (2011).
90. Ganz, T. Hepcidin , a key regulator of iron metabolism and mediator of anemia of inflammation Review article Hepcidin , a key regulator of iron metabolism and mediator of anemia of inflammation. **102,** 783–788 (2012).
91. Priotto, G. *et al.* Safety and effectiveness of first line eflornithine for *Trypanosoma brucei* gambiense sleeping sickness in Sudan: Cohort study. *Bmj* **336,** 705–708 (2008).
92. Kagira, J. M. *et al.* Prevalence and types of coinfections in sleeping sickness patients in Kenya (2000/2009). *J. Trop. Med.* **2011,** (2011).
93. Magez, S. & Caljon, G. Mouse models for pathogenic African trypanosomes: Unravelling the immunology of host-parasite-vector interactions. *Parasite Immunol.* **33,** 423–429 (2011).
94. Mons, B. & Sinden, R. E. Laboratory models for research in vivo and *in vitro* on malaria parasites of mammals: Current status. *Parasitol. Today* **6,** 3–7 (1990).
95. Wykes, M. N. & Good, M. F. What have we learnt from mouse models for the study of malaria? *Eur. J. Immunol.* **39,** 2004–2007 (2009).
96. Scheller, L. F., Wirtz, R. A. & Azad, A. F. Susceptibility of different strains of mice to hepatic infection with *Plasmodium berghei*. *Infect. Immun.* **62,** 4844–4847 (1994).
97. Gudisa, H. A Study on the Effect of Monomorphic *Trypanosoma brucei* rhodesiense, (Eatro 3 ET at 1.2) on Experimentally Infected Goats and Swiss White Mice. *J. Bacteriol. Parasitol.* **07,** (2016).
98. Janse, C. Life cycle of *Plasmodium berghei*. Available at: https://www.lumc.nl/org/parasitologie/research/malaria/berghei-model/life-cycle-berghei/#Sporozoites-and-pre-erythrocytic-development. (Accessed: 8th August 2018)
99. Mazurier, F. *et al.* A novel immunodeficient mouse model--RAG2 x common cytokine receptor gamma chain double mutants--requiring exogenous cytokine administration for human hematopoietic stem cell engraftment. *J. Interferon Cytokine Res.* **19,** 533–541 (1999).
100. Belizário, J. E. Immunodeficient Mouse Models: An Overview. *Open Immunol. J.* **2,** 79–85 (2009).
101. Engstler, M. & Boshart, M. Cold shock and regulation of surface protein trafficking convey sensitization to inducers of stage differentiation in *Trypanosoma brucei*. *Genes Dev.* **18,** 2798–2811 (2004).

102. Hirumi, H. & Hirumi, K. Continuous cultivation of *Trypanosoma brucei* blood stream forms in a medium containing a low concentration of serum protein without feeder cell layers. *J. Parasitol.* **75,** 985–989 (1989).
103. Franke-Fayard, B. *et al.* A *Plasmodium berghei* reference line that constitutively expresses GFP at a high level throughout the complete life cycle. *Mol. Biochem. Parasitol.* **137,** 23–33 (2004).
104. Janse, C. J. *et al.* High efficiency transfection of *Plasmodium berghei* facilitates novel selection procedures. *Mol. Biochem. Parasitol.* **145,** 60–70 (2006).
105. De Graaf, I. A. M. *et al.* Preparation and incubation of precision-cut liver and intestinal slices for application in drug metabolism and toxicity studies. *Nat. Protoc.* **5,** 1540–1551 (2010).
106. Ploemen, I. H. J. *et al.* Visualisation and quantitative analysis of the rodent malaria liver stage by real time imaging. *PLoS One* **4,** 1–12 (2009).
107. Douradinha, B. *et al.* Genetically attenuated P36p-deficient *Plasmodium berghei* sporozoites confer long-lasting and partial cross-species protection. *Int. J. Parasitol.* **37,** 1511–1519 (2007).
108. Mueller, A.-K. *et al. Plasmodium* liver stage developmental arrest by depletion of a protein at the parasite-host interface. *Proc. Natl. Acad. Sci. U. S. A.* **102,** 3022–7 (2005).
109. Mack, M. *et al.* Expression and Characterization of the Chemokine Receptors CCR2 and CCR5 in Mice. *J. Immunol.* **166,** 4697–4704 (2001).
110. Chromy, B. A., Fodor, I. K., Montgomery, N. K., Luciw, P. A. & McCutchen-Maloney, S. L. Cluster analysis of host cytokine responses to biodefense pathogens in a whole blood ex vivo exposure model (WEEM). *BMC Microbiol.* **12,** 1 (2012).
111. de Graaf, I. A. M. *et al.* Preparation and incubation of precision-cut liver and intestinal slices for application in drug metabolism and toxicity studies. *Nat. Protoc.* **5,** 1540–1551 (2010).
112. McGovern, K. E. & Wilson, E. H. Role of Chemokines and Trafficking of Immune Cells in Parasitic Infections. *Curr. Immunol. Rev.* **9,** 157–168 (2013).
113. Roffê, E. *et al.* Role of CCL3/MIP-1α and CCL5/RANTES during acute *Trypanosoma* cruzi infection in rats. *Microbes Infect.* **12,** 669–676 (2010).
114. Van Rooijen, N. & Sanders, A. Kupffer cell depletion by liposome-delivered drugs: Comparative activity of intracellular clodronate, propamidine, and ethylenediaminetetraacetic acid. *Hepatology* **23,** 1239–1243 (1996).
115. Nakashima, H. *et al.* Activation of CD11b+Kupffer Cells/Macrophages as a Common Cause for Exacerbation of TNF/Fas-Ligand-Dependent Hepatitis in Hypercholesterolemic Mice. *PLoS One* **8,** (2013).
116. Gottfried, E. *et al.* Expression of CD68 in non-myeloid cell types. *Scand. J. Immunol.* **67,** 453–463 (2008).
117. Yang, C. Y. *et al.* CLEC4F Is an Inducible C-Type Lectin in F4/80-Positive Cells and Is Involved in Alpha-Galactosylceramide Presentation in Liver. *PLoS One* **8,** (2013).
118. Hammond, M. D. *et al.* CCR2+Ly6Chi Inflammatory Monocyte Recruitment Exacerbates Acute Disability Following Intracerebral Hemorrhage. *J. Neurosci.* **34,** 3901–3909 (2014).
119. Geissmann, F., Jung, S. & Littman, D. R. Blood monocytes consist of two principal subsets with distinct migratory properties. *Immunity* **19,** 71–82 (2003).
120. Tsuji, M. *et al.* γδ T cells contribute to immunity against the liver stages of malaria in αβ T-cell-deficient mice. *Proc. Natl. Acad. Sci. U. S. A.* **91,** 345–349 (1994).

8. ANNEXES

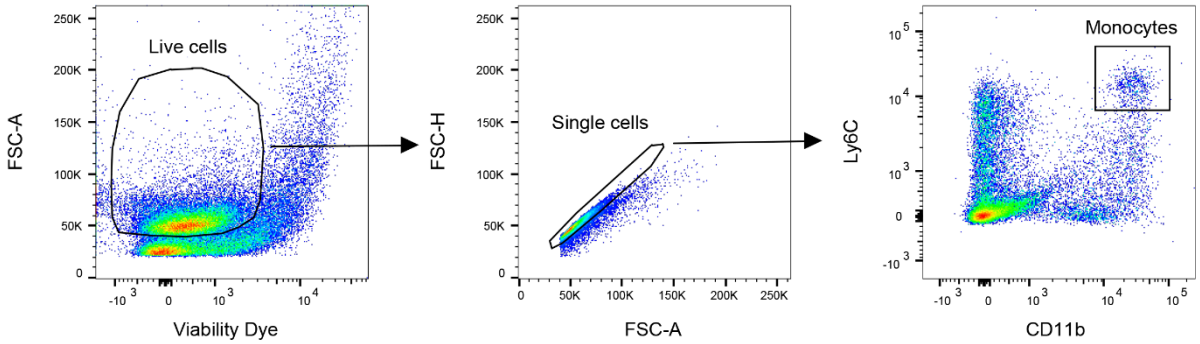

Supplementary Figure 1 – Gating strategy for flow cytometry analysis. Inflammatory monocytes show a high expression of LY6C and CD11b surface markers which allow their identification through flow cytometry analysis.

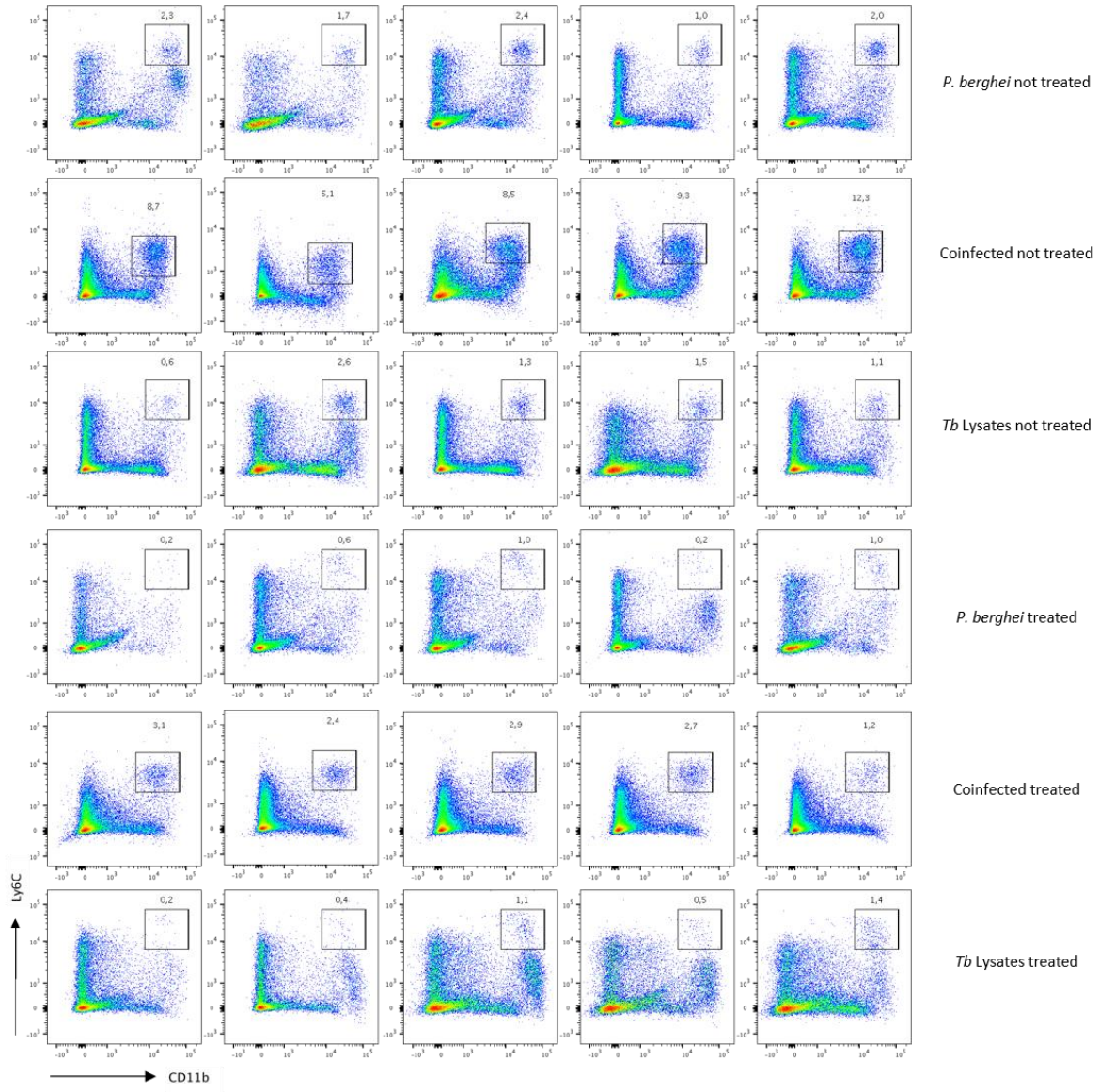

Supplementary Figure 2 – CD11b^{+}LY6C^{+} monocytes were successfully depleted with α-CCR2 antibody. Flow cytometry analysis of liver lymphocytes isolated from the livers of mice single infected with P. berghei, coinfected or injected with T. brucei lysates prior to infection, treated and not-treated with α-CCR2 antibody. Cells were assayed for expression of both CD11b and LY6C markers. Percentages of CD11b^{+}LY6C^{+} monocytes within the indicated gate are shown. Each row represents one individual from the indicated group on the left (n=5 mice per group).